Article

Theory of the low-temperature phases in boracites: latent antiferromagnetism, weak ferromagnetism, and improper magnetostructural couplings

TOLEDANO, Pierre, *et al*.

Abstract

A phenomenological theory of the magnetic and magnetoelectric properties of boracites is developed, using the Landau-Dzialoshinskii approach. An interpretation is proposed for the main distinctive features characterizing 11 members of this family of compounds. Three subclasses of materials are distinguished corresponding to 2 essentially different phys. situations. In Ni-I boracite the simultaneous ferromagnetic-ferroelectric-ferroelastic transition results from a nonlinear (improper) coupling of the magnetization, polarization, and strain components, to the primary order parameter identified as a "latent" antiferromagnetic ordering. Monoclinic Ni-I can be viewed as the 1st exptl. example of a new class of magnetic materials, which should be recognized macroscopically by an M .apprx. (Tc - T)3/2 variation law, the existence of a spontaneous structural ordering occurring simultaneously with the magnetic ordering, and a weak value of the magnetization despite its exchange origin. In the 2 other classes of trigonal and orthorhombic boracites, the transitions are purely magnetic, the order parameter having a 1- or [...]

Reference

TOLEDANO, Pierre, *et al*. Theory of the low-temperature phases in boracites: latent antiferromagnetism, weak ferromagnetism, and improper magnetostructural couplings. *Physical review. B, Condensed matter and materials physics*, 1985, vol. 32, no. 9, p. 6006-6038

DOI : 10.1103/PhysRevB.32.6006

Theory of the low-temperature phases in boracites: Latent antiferromagnetism, weak ferromagnetism, and improper magnetostructural couplings

P. Tolédano,* H. Schmid, M. Clin,* and J. P. Rivera
Département de Chimie Minérale, Analytique et Appliquée, Université de Genève, 30 quai Ernest-Ansermet, CH-1211, Genève 4, Suisse
(Received 1 February 1985)

A phenomenological theory of the magnetic and magnetoelectric properties of boracites is developed, using the Landau-Dzialoshinskii approach. An interpretation is proposed for the main distinctive features characterizing eleven members of this family of compounds, namely the symmetry changes, the magnetic and magnetoelectric anomalies, the nature of the order parameter, and its relationship with the relevant macroscopic components arising below T_c. Three subclasses of materials are distinguished corresponding to two essentially different physical situations. In Ni-I boracite the simultaneous ferromagnetic-ferroelectric-ferroelastic transition is shown to result from a nonlinear (improper) coupling of the magnetization, polarization, and strain components, to the primary order parameter identified as a "latent" antiferromagnetic ordering. The assumed monoclinic magnetic structure is formed by antiparallel noncompensating average spins of different magnitude, which differs from the usual ferrimagnetic order by the fact that only one type of magnetic ion is involved, which is found in equivalent positions in the cubic paramagnetic phase. Accordingly, Ni-I can be viewed as the first experimental example of a new class of magnetic materials, which should be recognized macroscopically by an $M\sim(T_c-T)^{3/2}$ variation law, the existence of a spontaneous structural ordering occurring simultaneously with the magnetic ordering, and a weak value of the magnetization despite its exchange origin. In the two other classes of trigonal and orthorhombic boracites, the transitions are assumed to be purely magnetic, the order parameter having a one- or two-dimensional antiferromagnetic order, bilinearly coupled to a weak magnetization of relativistic origin. The dielectric and elastic anomalies as well as the magnetoelectric properties in these two groups of boracites are explained by secondary couplings of the order parameter with the relevant nonspontaneous polar tensors. The complementarity of the two traditional Landau-type approaches of structural and magnetic transitions is illustrated.

I. INTRODUCTION

Since a series of papers[1–4] pointed out the ferroelectric, magnetic, and magnetoelectric properties of boracites, a large number of experimental studies have attempted to specify the structural and physical characteristics of more than 20 members of this family of compounds. Restricting ourselves to the best-known halide boracites (i.e., to boracites with general formula $M_3B_7O_{13}X$, where M=Mg,Cr,Mn,Fe,Co,Cu,Zn,Cd and X=Cl,Br,I), two distinctive features common to a large fraction of these compositions were initially verified:

(i) A ferroelectric-ferroelastic transition from the high-temperature $F\bar{4}3c$ (T_d^5) phase to a low-temperature orthorhombic $Pca2_1$ (C_{2v}^5) modification which involves a doubling of the cubic primitive unit cell.[5–7] Only three compounds do not undergo this structural change, namely the Cr-Br and Cr-I boracites[1,6] and the recently synthesized Cu-I boracite, which all remain cubic down to 4 K.

(ii) Except for Cu-I, all the compounds with M=Fe, Co, Ni, and Cu were shown to undergo transitions to magnetically ordered states[8] at lower temperatures ($T_c<61.5$ K). Furthermore, smooth magnetic anomalies which cannot be clearly connected with a phase transition were found for the series with M=Cr,[8] as well as for Ni-I boracite, for the latter one around 120 K.

Although the preceding data suggested an apparently homogeneous behavior among the boracite family, further studies revealed a relatively complex variety of situations within each of the two categories (structural and magnetic) of transitions. Thus in four compounds (Fe-Cl, Co-Cl, Zn-Cl, and Fe-I) the following sequence of phases was identified:[9–11] $F\bar{4}3c\rightarrow Pca2_1\rightarrow Pb\rightarrow R3c$. The trigonal phase was also found in Fe-Br, whereas a monoclinic phase (but no trigonal phase) was observed in the Cr-Cl boracite.[12] In Ni-I, the crystal was shown to remain cubic down to 61.5 K where the structural and magnetic transitions occur simultaneously from the cubic phase to a monoclinic phase.[13,14]

Beyond the structural diversity of boracites, dielectric and calorimetric results brought to light striking differences among their transition anomalies. Thus for Ni-I,[14] Mn-I, and Cu-Cl,[15,16] the dielectric constant ϵ has a downward jump on heating, whereas in Cu-Br,[17] Mg-Cl,[18] or Co-I,[19] the jump is upward. The temperature dependence of the spontaneous polarization $P_s(T)$ is appreciably different in compounds such as Ni-Br (Ref. 20) and Mg-Cl (Ref. 21) on the one hand, and Co-I (Ref. 22) or Fe-I (Ref. 23) on the other hand. Moreover, the magni-

tude of P_s is about two orders smaller in Ni-I (7.6×10^{-4} $C\,m^{-2}$) (Ref. 14) than in Fe-I (3.9×10^{-2} $C\,m^{-2}$).[24] Similarly, while in a large number of boracites the cubic to orthorhombic transition has a pronounced first-order character,[25] it seems to be closer to second-order in compounds such as Mn-I (Ref. 26) or Cu-Cl.[27,28]

The situation appears to be equally complex for the magnetic class of transitions. Among the eleven members of the boracite family in which a magnetic order was confirmed,[3,8] at least four different types of transitions from paramagnetic to ferro- or antiferromagnetic phases have been reported, namely $\bar{4}3m\,1'\rightarrow m'$ for Ni-I boracite,[14] $mm\,21'\rightarrow m'm\,2'$ for Co-Br,[29] $mm\,21'\rightarrow mm\,2$ for Ni-Cl,[30] and $3m\,1'\rightarrow m$ for Co-Cl.[31] While the existence of only one magnetic transition is known so far for Fe-Cl,[31] Co-Cl,[9,31] Fe-Br,[31] Co-Br,[29] Cu-Br,[3] and Fe-I,[8] evidence for two successive magnetic phases close to each other in temperature is found in Ni-Cl,[30,32] Ni-Br,[20,30] and Co-I.[33] A spontaneous Faraday effect showing the existence of a weak magnetization so far has been observed in five compounds (Co-Br, Co-Cl, Ni-Br, Ni-Cl, and Ni-I), the temperature variations of the Faraday rotation angle and magnetization revealing a variety of surprising behaviors (see for instance the curves in Refs. 12, 20, 30, and 34). A magnetoelectric effect was detected for Ni-Br,[20] Ni-Cl,[32] Ni-I,[4] Cu-Cl,[35] Co-Cl,[31] Fe-Br, and Fe-Cl,[31] with remarkable shapes for the magnetoelectric coefficients.

On theoretical grounds, a number of phenomenological models have attempted to explain the structural[36–39] and magnetic[40–44] transitions in boracites. Although each of these models partly clarifies some basic features of a given subclass of compounds (see discussion in the following sections), they fail to account successfully for the entire set of experimental data, as they seem to have neglected some essential peculiarities of the boracite family. It is the aim of the present work to present a theory of boracites which accounts for the variety of situations that were briefly outlined above. As the magnetic and magnetostructural low-temperature transitions are, to a great extent, disconnected from the purely structural transitions which take place at higher temperatures, the theory will be exposed in two separate papers. The present study deals with the set of magnetic transitions occurring from $T_c=61.5$ K (i.e., in Ni-I boracite) down to $T_c\sim7$–10 K (in Ni-Cl and Cu-Cl boracites). A planned subsequent article will consider the structural transitions taking place in the temperature range $T_c=190$ K (Co-I) to $T_c=795$ K (Cd-Cl).

This paper is organized as follows. In Sec. II, a Landau theory of magnetic and magnetostructural transitions is developed, which explains the low-temperature sequence of transitions as resulting from an *improper* or *pseudoproper* coupling of the order parameter, identified as an antiferromagnetic ordering of the magnetic moments, to the various macroscopic quantities[45] (i.e., magnetization, polarization, and strain). In the framework of the aforementioned model, three subclasses of magnetic boracites are distinguished. Their magnetic, dielectric, elastic, and magnetoelectric features are examined successively in Secs. III, IV, and V. Finally, the fundamental interactions and mechanisms responsible for the magnetic properties of boracites are discussed in Sec. VI, with reference to Dzialoshinskii theories of weak ferromagnetism[46] and latent antiferromagnetism.[47]

II. LANDAU THEORY OF MAGNETIC AND MAGNETOSTRUCTURAL TRANSITIONS IN BORACITES

A. Classification of the observed sequences of symmetry changes

The symmetry modifications occurring in the boracites in which magnetic phases have been observed, are summarized in Table I [column (b)]. In this table one can see [column (c)] that the occurrence of magnetic transitions for all the listed materials, is firmly established by a number of experimental results, such as the detection of a spontaneous Faraday effect, a magnetic hysteresis loop, or clearcut anomalies in the magnetic susceptibility. On the other hand, a strong connection between the magnetic transition and the dielectric or elastic properties is in some cases revealed by the existenced of marked variations of the spontaneous polarization or elastic constants [column (d)] and by a magnetoelectric signal. However it can be noted that identification of the magnetic symmetries is not deduced from neutron diffraction studies but from a set of optical observations which include essentially the ferromagnetic-ferroelectric domain pattern under the conjugated effect of applied magnetic and electric fields, together with the probing of the tensorial properties of the magnetoelectric effect. Such observations allow to determine only the magnetic classes of the phases and not their Shubnikov space groups. In this respect, the materials listed on Table I correspond to three types of symmetry modifications.

(1) Nickel-iodine boracite is a unique example of boracite in which a magnetic and structural transition occurs directly from the paramagnetic $F\bar{4}3c\,1'$ phase to a monoclinic phase of magnetic class m'. The absence of other transitions, the consistency of the preceding symmetries and the simultaneity of the onset of weak ferromagnetism and ferroelectricity have been demonstrated by magnetic,[14] dielectric,[14] magnetoelectric,[4] piezoelectric,[48] and birefringence[14] measurements. It is noteworthy that the smooth anomalies of various physical properties found around 120 K,[4,49–51] or below the 61.5-K transition,[52,53] have been shown recently to be associated with relaxation mechanisms due to defects[48,54] and not with a structural transition, as was claimed by some authors.[41,55]

(2) A second subclass of magnetic boracites is formed by Fe-Cl, Fe-Br, Fe-I, and Co-Cl boracites. In these compounds a paramagnetic-ferromagnetic transition takes place corresponding to a $3m\,1'\rightarrow m$ symmetry change. In the Fe-X compositions the monoclinic group requires confirmation, though the ferromagnetic-ferroelectric character of the phase transition is evidenced by a magnetic hysteresis loop[8] and susceptibility[3] and magnetoelectric[31] measurements. In the Co-Cl boracite the magnetic properties[31] and the ferromagnetic-ferroelectric domain pattern clearly identify the Shubnikov class of symmetry m.[56]

(3) In a third group of materials, the magnetically or-

TABLE I. Phase transition in magnetic boracites. For each compound [listed in column (a)] the following features are given. Column (b) indicates the sequence of structural and magnetic transitions and the symmetries of the corresponding phases, using the Shubnikov notation (Ref. 61). Column (c) gives the available data illustrating their magnetic properties. The values for the magnetization and coercive field are given at 4.2 K. Column (d) shows the structural anomalies connected with the magnetic transitions, and the evidence for magnetoelectric properties (ME).

(a)	(b)	(c)	(d)
Ni-I	$F\bar{4}3c\,1' \overset{61.5\,K}{\leftrightarrow} m'$	Faraday rotation,[a,b] magnetization,[c,d] hysteresis,[e] susceptibility,[f,a] ferromagnetic domains,[a,b] neutron diffraction,[g,h] $\mu=0.016$ emu/g$=0.9$ G,[d,i] $H_c=4000$ Oe[j]	ME,[a,k,l,m] ferroelectric domains,[n] birefringence,[b] polarization,[a,b] dielectric permittivity,[a,b,o] elastic const.[p,q]
Fe-Cl	$F\bar{4}3c\,1' \overset{610\,K}{\leftrightarrow} Pca2_11' \overset{543\,K}{\leftrightarrow} m\,1' \overset{528\,K}{\leftrightarrow} R\,3c\,1' \overset{10.5\,K}{\leftrightarrow} (m)$	hysteresis,[j] susceptibility,[f,r] $\mu=5.8$ emu/g$=258$ G,[j] $H_c=170$ Oe[j]	ME,[r,s] ferroelectric domains[s]
Fe-Br	$F\bar{4}3c\,1' \overset{495\,K}{\leftrightarrow} Pca2_11' \overset{405\,K}{\leftrightarrow} R\,3c\,1' \overset{18\,K}{\leftrightarrow} (m)$	hysteresis,[j] $\mu=7.9$ emu/g$=414$ G,[j] $H_c=1500$ Oe[j]	ME[r]
Fe-I	$F\bar{4}3c\,1' \overset{349\,K}{\leftrightarrow} Pca2_11' \underset{218\,K}{\overset{203\,K}{\rightleftarrows}} m\,1' \underset{205\,K}{\overset{191\,K}{\rightleftarrows}} R\,3c\,1' \overset{30\,K}{\leftrightarrow} (m)$	hysteresis,[j] susceptibility,[f] $\mu=2.6$ emu/g$=137$ G,[j] $H_c=9500$ Oe[j]	
Co-Cl	$F\bar{4}3c\,1' \overset{623\,K}{\leftrightarrow} Pca2_11' \overset{538\,K}{\leftrightarrow} m\,1' \overset{468\,K}{\leftrightarrow} R\,3c\,1' \overset{9-11\,K}{\leftrightarrow} m$	Faraday rotation,[t] susceptibility,[f,r] ferromagnetic domains,[s] $\mu=8.8$ emu/g$=419$ G,[j], $H_c=300$ Oe[j]	ME,[r,s] ferroelectric domains[s]
Co-Br	$F\bar{4}3c\,1' \overset{466\,K}{\leftrightarrow} Pca2_11' \overset{16\,K}{\leftrightarrow} m'm2'$	Faraday rotation,[u] susceptibility,[f] ferromagnetic domains,[u] $\mu=9.5$ emu/g$=482$ G,[j] $H_c=300$ Oe[j]	birefringence[u]
Co-I	$F\bar{4}3c\,1' \underset{198\,K}{\overset{190\,K}{\rightleftarrows}} Pca2_11' \overset{38\,K}{\leftrightarrow} (?) \overset{29\,K}{\leftrightarrow} (?)$	magnetization,[v] susceptibility,[f] neutron diffraction,[w] $\mu=1.7$ emu/g$=94$ G,[j] $H_c=3500$ Oe[j]	ME,[x] dielectric permittivity,[y,v]
Ni-Cl	$F\bar{4}3c\,1' \underset{610\,K}{\overset{608\,K}{\rightleftarrows}} Pca2_11' \overset{25\,K}{\leftrightarrow} mm2 \overset{8-10\,K}{\leftrightarrow} m'm2'$	Faraday rotation,[z] susceptibility,[f,aa] ferromagnetic domains,[z] magnetization,[aa] magnetic torque,[aa] $H_c(T)$,[bb] $\mu=0.4$ emu/g$=19$ G,[j] $H_c=300$ Oe[j]	ME,[bb] birefringence[z]
Ni-Br	$F\bar{4}3c\,1' \underset{399\,K}{\overset{398\,K}{\rightleftarrows}} Pca2_11' \overset{30\,K}{\leftrightarrow} (?) \overset{16.8\,K}{\leftrightarrow} m'm2'$	Faraday rotation,[z] susceptibility,[f] ferromagnetic domains,[z] $H_c(T)$,[cc] $\mu=2.15$ emu/g$=111$ G,[j] $H_c=1350$ Oe[j]	ME,[cc] ferroelectric domains,[z] polarization[cc]

TABLE I. (*Continued*).

(a)	(b)	(c)	(d)
Cu-Cl	$F\bar{4}3c\,1' \overset{369\,K}{\leftrightarrow} Pca2_1 1' \overset{8.4\,K}{\leftrightarrow} m'm'2$	magnetic torque,[dd,t] $\mu=0.015$ emu/g^{i}=(0.078^{dd})=0.08 G	ME,[dd,t]
Cu-Br	$F43c\,1' \overset{243\,K}{\leftrightarrow} Pca2_1 1' \overset{24\,K}{\leftrightarrow} (?)$	susceptibility,[f] $\mu=0.08$ emu/g=4.06 G;[j] $H_c=800$ Oe[j]	dielectric permittivity,[y] polarization[y]

[a] Reference 4. [f] Reference 3. [k] Reference 6. [p] Reference 51. [u] Reference 29. [z] Reference 30.
[b] Reference 14. [g] Reference 82. [l] Reference 13. [q] Reference 54. [v] Reference 33. [aa] Reference 57.
[c] Reference 34. [h] Reference 83. [m] Reference 99. [r] Reference 31. [w] Reference 84. [bb] Reference 32.
[d] Reference 91. [i] Reference 112. [n] Reference 43. [s] Reference 56. [x] Reference 44. [cc] Reference 20.
[e] Reference 92. [j] Reference 8. [o] Reference 48. [t] Reference 58. [y] Reference 17. [dd] Reference 35.

dered phases arise below a phase of orthorhombic $Pca2_11'$ symmetry. In Ni-Cl a sequence of two magnetic phases has been found:[32,57] an antiferromagnetic phase of Shubnikov group $mm2$, followed by a weak ferromagnetic phase of symmetry $m'm2'$. Two successive phases with nonzero magnetization occur in Ni-Br and Co-I boracites. In Co-Br, a single ferromagnetic phase is observed below the paramagnetic $Pca2_11'$ phase. In this material spontaneous Faraday rotation and the ferromagnetic domain pattern are consistent with the $m'm2'$ Shubnikov group.[29] In Cu-Br, a very weak magnetic moment[8] attests to the ferromagnetic nature of the phase arising at 24 K, the symmetry of which remains to be determined. Finally, for Cu-Cl, two distinct transition temperatures are reported.[8,35] Haida *et al.*[35] propose a $m'm'2$ Shubnikov group for the ferromagnetic phase below 8.4 K, at variance with the earlier supposition of an $m'm2'$ symmetry.[8,56]

It can be pointed out that the Cr-X boracites have not been included in Table I as only smooth anomalies in the magnetic susceptibilities have been reported up to now for this series of materials, but no clear proof for the existence of magnetic transitions has been given. On the other hand, unpublished results on Cr-Cl (Ref. 58) suggest that chromium boracites could experience a fourth type of magnetic transition with a *monoclinic* paramagnetic phase. However, more experimental data are needed for a theoretical approach to this group of compounds.

B. Identification of the order-parameter symmetries in the boracite family

The first step for developing a Landau theory of magnetic boracites is to determine for each material the relevant *parent* phase, i.e., the high-temperature paramagnetic phase to which belongs the irreducible corepresentation (IC) inducing the magnetic transition(s). For Ni-I boracite the parent-paramagnetic phase can be unambiguously identified as the $F\bar{4}3c\,1'$ phase, as on one hand it corresponds to the only stable phase evidenced above the transition at $T_c=61.5$ K, and on the other hand the domain pattern observed below T_c shows the existence of twelve ferroelectric domains and twenty-four ferromagnetic domains. The number and orientations of both types of domain, schematized on Fig. 1 are consistent, respectively, with the structural $\bar{4}3m\,1'\rightarrow m\,1'$ and magnetic $\bar{4}3m\,1'\rightarrow m'$ symmetry modifications.

The choice of the parent phase for the two other groups of boracites listed on Table I is less obvious, as the ferroelectric and ferromagnetic phases take place in separated stages. Thus in Co-Br,[29] as a representative of the group of orthorhombic boracites, six ferroelectric domains appear first at 466 K, according to the $\bar{4}3m\,1'\rightarrow mm\,21'$ point group change. Then, below 16 K, twelve ferromagnetic domains can be observed (Fig. 2). This can be connected either with a $mm\,21'\rightarrow m'm\,2'$ point-group change (i.e., two ferromagnetic domains being distinguished in each ferroelectric domain) or with an indirect $\bar{4}3m\,1'\rightarrow m'm\,2'$ modification. An analogous situation is encountered in Co-Cl, which is illustrative of the subclass of trigonal boracites, where twenty-four ferromagnetic domains are evidenced below 9 K (Ref. 59) (Fig. 3). This

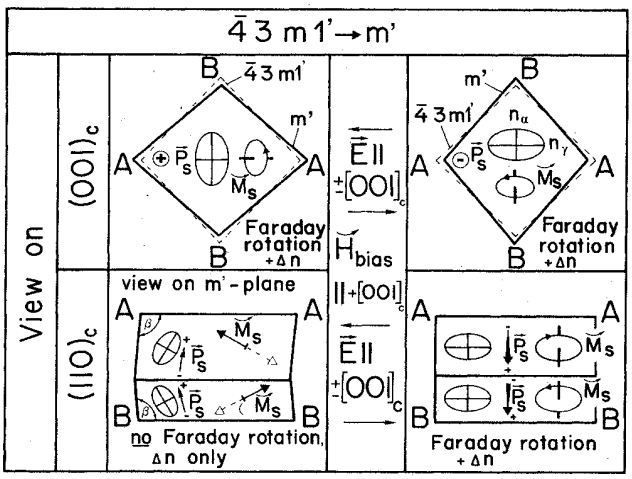

FIG. 1. Domain pattern in the monoclinic Cc' phase of Ni-I boracite. Representation of four among the 24 possible ferroelectric-ferroelastic-ferromagnetic domain states are shown. Each of the four domains is represented as a ferromagnetic single domain in agreement with a magnetic bias field **H** assumed parallel to $[001]_c$. Within the m' plane (lower left-hand case) the vectors $\mathbf{P}_s, \mathbf{M}_s$ and the indicatrix principal section (b axis perpendicular), occupy three arbitrary orientations that may change with temperature. The letters A and B designate the opposite polarity of the corners of the cubic $\bar{4}3m$ conventional (F) cell. The AB corners are kept immobile for all domains represented. Electric field reversal along $\pm[001]_c$ does not lift the degeneracy in layers of monoclinic domains that are distinguishable on $(110)_c$ only (lower cases). Assuming $(001)_c$ composition planes, the four ferroelectric-ferroelastic domains are indistinguishable on $(001)_c$ cuts (upper cases) because of identical indicatrix cross section. On $(110)_c$ cuts two of the states are distinguishable owing to difference in extinction directions (lower left-hand case) and the two other ones (lower right-hand case) owing to opposite Faraday rotation for a magnetic bias **H** parallel to $\pm[001]$, despite identical indicatrix cross section.

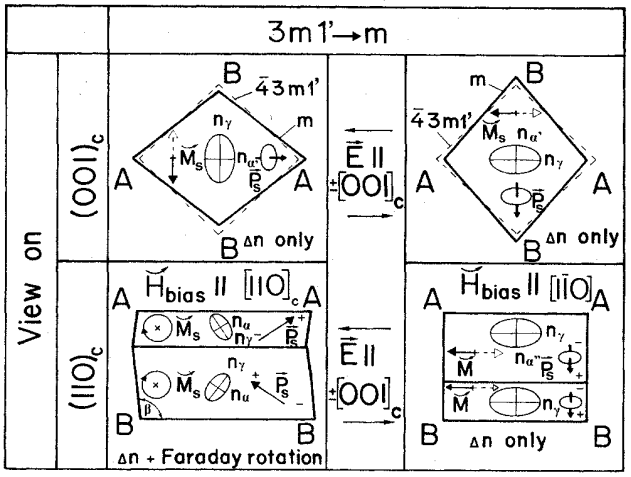

FIG. 2. Domain pattern in the monoclinic Cc phase of trigonal boracites (e.g., Co-Cl). Representation of four of the 24 domain states. Only four ferroelectric-ferroelastic domains are possible, to each of which belong six different states of the spontaneous magnetization $\mathbf{M}_s$. Only one orientation of $\mathbf{M}_s$ is indicated in every ferroelectric-ferroelastic domain, in agreement with a magnetic bias field parallel to $[110]_c$ and $[1\bar{1}0]_c$. Two of the four ferroelectric domains are distinguishable on $(110)_c$ (lower left-hand case) owing to different extinctions. The two other ones are only distinguishable by tilting round the refractive index n_γ, creating differences in $n_\gamma - n_\alpha$ on $(110)_c$ (lower right-hand case). Electric field reversal parallel to $\pm[001]_c$ interchanges lamellar domain packages in a similar way as in the symmetry change $\bar{4}3m\ 1' \rightarrow m'$.

may result either from a direct $3m\,1' \rightarrow m$ symmetry lowering (i.e., the crystal remains crystallographically trigonal[60] and six inequivalent ferromagnetic domains are found within each of the four already existing ferroelectric domains) or from an indirect $\bar{4}3m\ 1' \rightarrow m$ transition.

The preceding ambiguity on the choice of the paramagnetic phase for the Co-Br and Co-Cl types of boracites, can be removed through a Landau group-theoretical analysis of the phase transitions which are liable to arise below each of the three paramagnetic groups $Pca2_11'$, $R3c1'$, and $\bar{F}43c1'$. Such as analysis also allows the identification of the order-parameter symmetries corresponding to the phase transitions reported in Table I.

The specific procedure for applying the Landau theory to transitions from a paramagnetic phase using the Shubnikov groups[61] and their corepresentations[62,63] has been explicited in a number of studies.[64–68] It involves three steps. In the first place the "active" IC's[69] of the paramagnetic Shubnikov group, denoted G_0, are selected on the basis of the Lifshitz symmetry criterion[70] (the Landau condition[70] being automatically satisfied). The selection determines a few stars k^* in the magnetic Brillouin zone[63] of G_0 and certain small corepresentations[69] τ_n of the group $G_{\mathbf{k}}$ of the **k**-vector representative of k^*. The order-parameter expansion associated with the IC is then constructed and its minima specified as a function of the expansion coefficients. Finally, the symmetry change $G_0 \rightarrow G$ corresponding to each minimum is worked out.

The results of the application of the Landau theory to the three Shubnikov groups $Pca2_11'$, $R3c1'$, and $F\bar{4}3c1'$, are summarized in Tables II and III. Table II gives for each of the considered paramagnetic groups, the ferromagnetic and antiferromagnetic groups [columns (c) and (d)] induced by the IC's fulfilling the Lifshitz condition, together with the symmetry characteristics of the corresponding order parameters [columns (e) and (f)]. The labeling of column (g) refers to the order-parameter expansions $F_1(\alpha,\eta_i,\beta_k)$ which are explicited up to the fourth degree in Table III. The equilibrium values of the order parameter in each low-symmetry phase, as well as the corresponding range of values of the expansion coefficients are expressed in columns (c) and (d) of Table III. For sake of completeness, the point groups induced by "inactive" IC's of selected high-symmetry points of the Brillouin-zone surfaces are also indicated in Table II.

A comparison of the theoretical results given in Table

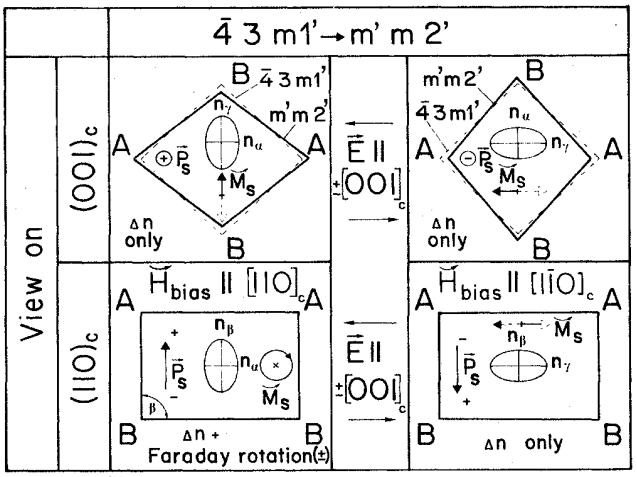

FIG. 3. Domain pattern in the orthorbombic $Pc'a2_1'$ phase (e.g., Ni-Cl, Co-Br) of boracites. Two out of the six possible ferroelectric-ferroelastic domains are represented. They have opposite directions of $\mathbf{P}_s$ (parallel to $[001]_c$ and are related by the lost symmetry operations $\bar{4}$. Interchange is possible by means of an electric field $\mathbf{E}\|\pm[001]$. The spontaneous strain tensor [shear in $(001)_c$ plane], the optical indicatrix (principal indices $n_\alpha, n_\beta, n_\gamma$), and the orthorhombic a,b axes are related by a 90° rotation. Each ferroelectric domain can split up in two ferromagnetic domains with $\pm M_s \| n_\gamma$. The four ferroelectric single domains are represented as ferromagnetic domains due to a bias field $\mathbf{H}$ assumed parllel to $[110]_c$ and $[1\bar{1}0]_c$. For the $(110)_c$ cut with $\mathbf{M}_s$ perpendicular to the cut, spontaneous birefringence Δn and Faraday rotation are superposed. The ferromagnetic domains will be visible only in case of a high $M_s/\Delta n$ ratio.

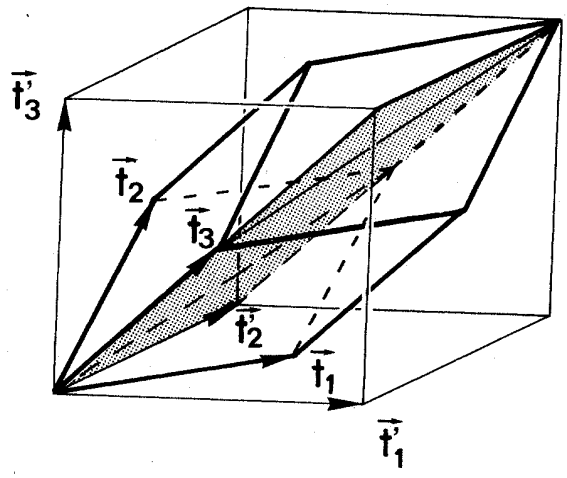

FIG. 4. Lattice modification at the $F\bar{4}3c\,1' \rightarrow Cc'$ transition assumed for Ni-I boracite. The monoclinic cell contains *four* cubic primitive cells. The magnetic *and* crystallographic monoclinic cells have the same primitive translations: $\mathbf{t}_1' = \mathbf{t}_1 - \mathbf{t}_2 + \mathbf{t}_3$, $\mathbf{t}_2' = \mathbf{t}_1 + \mathbf{t}_2 - \mathbf{t}_3$, $\mathbf{t}_3' = -\mathbf{t}_1 + \mathbf{t}_2 + \mathbf{t}_3$.

II with the experimental data of Table I, leads to the following conclusions.

1. The paramagnetic to ferromagnetic $F43c1' \rightarrow m'$ symmetry change observed in nickel-iodine boracite can be unequivocally related to the six-dimensional IC labeled τ_1 at the X point of the face-centered-cubic lattice. Actually, as it can be seen in Table II, the other IC's of the $F\bar{4}3c\,1'$ group lead either to antiferromagnetic groups or to ferromagnetic groups of symmetry distinct from m'. Moreover, the change in magnetic structure induced by τ_1 has the remarkable property of being necessarily connected with a structural transition,[45] a feature which is verified in Ni-I boracite.

In Fig. 4 we have represented schematically the magnetostructural lattice change corresponding to the $F\bar{4}3c\,1' \rightarrow Cc'$ transition. It involves a quadrupling of both the magnetic and crystallographic unit cell. In this respect, one must keep in mind that the magnetic symmetry of a paramagnetic crystal (the grey Shubnikov group) embodies its structural symmetry (the Fedorov group) in such a manner that the IC's of the paramagnetic group depict not only the degrees of freedom of the spin distribution, but also an eventual motion of the atoms in the crystal. This latter situation has been shown to be realized only for a small minority of zone-boundary IC's, the larger number of IC's inducing a purely magnetic modification.[45,60,68] Thus, it can be noted from Table II, that among the whole set of IC's of the $F43c\,1'$ group, only those IC's at the X point which correspond to a fourfold increase of the paramagnetic cell, involve necessarily a structural change.[60] The distinctive feature of this recently identified type of magnetostructural transition,[45,68] which differs in many respects from the mere magnetostriction,[60] is discussed in Secs. III and VI, in the light of the experimental data on Ni-I boracite.

One can also note that the Cc' ferromagnetic group displays, on a theoretical ground, the remarkable characteristic to be a *nonmaximal subgroup*[71] of the $F43c\,1'$ paramagnetic group. This property, established in Appendix A, should make nickel-iodine boracite the first experimental counterexample of the maximal subgroup rule[72] conjectured for phase transitions involving a group-subgroup relationship between the phases. A theoretical counterexample was already pointed out in Ref. 73.

The set of distinct six-dimensional matrices corresponding to the $\tau_1(X)$ IC [i.e., the image of the IC (Ref. 74)] is given in Appendix B. It allows to construct the order-parameter expansion associated with the $F\bar{4}3c\,1' \rightarrow Cc'$ transition. This expansion, labeled d in Table III, differs from the one considered by Dvorak and Petzelt[36] and by Gufan and Sakhnenko[38] for the structural transitions in boracites, by the absence of a third-degree invariant, which vanishes, in our model, under the effect of the time-reversal operator. Thus the 61.5-K magnetostructural transition in Ni-I boracite may occur as a second-order transition (see discussion in Sec. III). It can be also

TABLE II. Results of the Landau symmetry analysis for the active (Ref. 69) IC's of the paramagnetic groups $Pca\,2_1 1'$, $R\,3c\,1'$, and $F\bar{4}3c\,1'$. Column (a) paramagnetic groups. (b) High-symmetry points of the paramagnetic Brillouin zones labeled as the corresponding points of the crystallographic Brillouin zones in the notations of Zak *et al.* (Ref. 20) and Kovalev (Ref. 109). (c) Ferromagnetic (F) and anitferromagnetic (AF) low-symmetry groups. Each IC (in parentheses) is specified as the corresponding irreducible representation (Ref. 109) from which it is constructed. (d) Primitive translations and antitranslations of the primitive unit cell in the low-temperature phase, with reference to the paramagnetic primitive translations. (e) Finite groups of distinct matrices (images) forming the IC's, specified as in Ref. 121. (f) Order-parameter dimension. (g) Order-parameter expansion type in reference to Table III. The point groups and type of magnetic ordering induced by some relevant inactive IC's of the three paramagnetic groups are also reported.

(a)	(b)	(c)	(d)	(e)	(f)	(g)
$Pca\,2_1 1'$	$\Gamma(k_{19})$	AF $Pca\,2_1(\tau_1)$ F $Pc'a'2_1(\tau_2), Pca'2_1'(\tau_3), Pc'a\,2_1'(\tau_4)$	$t_1,t_2,t_3(V)$	C_i	1	a
	$Y(k_{21})$	AF $P_bca\,2_1(\tau_1,\tau_3), P_bna\,2_1(\tau_2\tau_4)$	$t_1,2t_2,t_3;Rt_2(2V)$			
	$X(k_{20}), Z(k_{22})$ $T(k_{23}), U(k_{24})$ $S(k_{25}), R(k_{26})$	AF$\neq$Lifshitz: $M_0P_a(m,2)$			(2)	
$R\,3c\,1'$	$\Gamma(k_7)$	AF $R\,3c(\tau_1)$ F $R\,3c'(\tau_2)$ $F(\mathrm{I}\,Cc\,\mathrm{II}\,Cc')(\tau_3)$	$t_1,t_2,t_3(V)$	C_i	1	a
			$t_1,t_1+t_2,t_3(V)$	C_{6v}	2	b
	$X(k_5)$	AF $\mathrm{I}\,P_Ac(\tau_1,\tau_2)$ AF $\mathrm{II}\,R\,3c(\tau_1)$ F $\mathrm{II}\,R\,3c'(\tau_2)$	$\begin{Bmatrix} t_2\pm t_3, t_1+t_2+t_3 \\ Rt_2, Rt_3 \end{Bmatrix}(2V)$ $t_3\pm t_2\mp t_1, t_2-t_3+t_1(4V)$	O_H	3	c
	$A(k_4), Z(k_8)$	AF$\neq$Lifshitz: tri.$P_s(1), R_I(3)$			(2,4,6)	
$F\bar{4}3c\,1'$	$\Gamma(k_{11})$	AF $F\bar{4}3c(\tau_1), F\bar{4}'3c'(\tau_2)$ AF $(\mathrm{I}\,I\bar{4}c\,2, \mathrm{II}\,I\bar{4}'c'2)(\tau_3)$ AF $(\mathrm{I}\,I\bar{4}'c\,2', \mathrm{II}\,R\,3c)(\tau_4)$ F $(\mathrm{I}\,I\bar{4}c'2', \mathrm{II}\,R\,3c')(\tau_5)$	$t_1,t_2,t_3(V)$	C_i C_{6v} O_H	1 2 3	a b c
	$X(k_{10})$	AF $\mathrm{I}\,P_I\bar{4}c\,2(\tau_2,\tau_5), P_I\bar{4}b\,2(\tau_3,\tau_4)$ AF $\mathrm{II}\,P\bar{4}3n(\tau_2,\tau_5), P\bar{4}'3n'(\tau_3,\tau_4)$	$\begin{Bmatrix} t_2-t_1, t_3, t_1+t_2-t_3 \\ Rt_1, Rt_2 \end{Bmatrix}(2V)$ $\begin{Bmatrix} t_1\pm t_2+t_3 \\ t_2+t_3-t_1 \end{Bmatrix}(4V)$	O_H	3	c
		AF $\mathrm{I}\,P_Ic\,2_1a, \mathrm{II}\,C_A222_1$ AF $\mathrm{III}\,P\bar{4}2_1c, \mathrm{IV}\,P2_13, \mathrm{V}\,R\,3c$ F $\mathrm{VI}\,R\,3c', \mathrm{VII}\,Cc', \mathrm{VIII}\,Cc$ (τ_1)	$\begin{Bmatrix} t_2-t_1, t_3, t_1+t_2-t_3 \\ Rt_1, Rt_2 \end{Bmatrix}(2V)$ $\begin{Bmatrix} t_1\pm t_2\mp t_3 \\ t_2+t_3-t_1 \end{Bmatrix}(4V)$	L_7	6	d
	$W(k_8), L(k_9)$	AF$\neq$Lifshitz cub.F_s and $P_I(23), R_I(3)$ortho.$I_c(222)$ tetr.$I_c(\bar{4}2m,4), M_oC_c(m,2)$			(8,12,16)	

stressed that our model differs strongly from the Landau-type descriptions given in Refs. 40–44 and Ref. 75 for the magnetic transition in Ni-I. In these models, an orthorhombic symmetry is assumed for the low-temperature phase, the 61.5-K transition being considered as a purely magnetic one (with a separate structural transition at 120 K) and connected to a three-dimensional irreducible representation at the center of the face-centered cubic Brillouin zone. The recent experimental data on Ni-I boracite, as well as the above-mentioned symmetry analysis disprove such an explanation.

2. *The R3c1′→m modification evidenced in Co-Cl—type boracites can be obtained either from a two-dimensional IC (denoted τ_3 in Table II) at the center of the trigonal Brillouin zone,* or from the same IC of the $F43c\,1'$ group as for Ni-I boracite. However, this latter possibility must be discarded as it would involve a structural transition to occur simultaneously with the magnetic ordering. This is in contrast with the observation of an essentially unchanged trigonal ferroelectric domain structure in Co-Cl below the 9-K ferromagnetic transition.[59] Thus the parent phase for the Co-Cl group of ferromagnetic boracites should be chosen as the $R\,3c\,1'$ phase. Accordingly the ferromagnetic phase corresponds to the Cc Shubnikov group with a unit cell containing the same number of atoms as the trigonal cell. Let us stress that the $R\,3c\,1'\rightarrow Cc$ transition may induce a slight structural distortion (undetected up to now in Co-Cl) through an interaction of the magnetostrictive type.[60] A group theoretical analysis[76] shows that the crystallographic symmetry of the ferromagnetic phase should then be lowered to a triclinic symmetry 1.

TABLE III. Order-parameter expansions F_1 associated to the IC's considered in Table II. Labeling (a) and explicit form (b) of the expansions. (c) Equilibrium values for the order parameter components in the low-temperature phases, and (d) stability conditions fulfilled by the expansion coefficients.

(a)	(b)	(c)	(d)
$F_1=a$	$\frac{\alpha}{2}\eta^2+\frac{\beta}{4}\eta^4$	$\eta\neq 0$	$\beta>0$
$F_1=b$	$\frac{\alpha}{2}\rho^2+\frac{\beta}{4}\rho^4+\frac{\gamma_1}{6}\rho^6$ $+\frac{\gamma_2}{6}\rho^6\cos 6\psi\ (\eta_1=\rho\cos\psi,\ \eta_2=\rho\sin\psi)$	I $\psi=0,\rho\neq 0$	$\beta_1>0,\gamma_2<0$
		II $\psi=\frac{\pi}{2},\rho\neq 0$	$\beta_1>0,\gamma_2>0$
$F_1=c$	$\frac{\alpha}{2}\sum_{i=1,3}\eta_i^2+\frac{\beta_1}{4}\sum_{i=1,3}\eta_i^4$ $+\frac{\beta_2}{2}\sum_{\substack{i=1,3\\ i<j}}\eta_i^2\eta_j^2$	I $\eta_1\neq 0,\eta_2=\eta_3=0$	$\beta_2>\beta_1>0$
		II $\eta_1=\eta_2=\eta_3\neq 0$	$\beta_1>0,\beta_1>\beta_2>-\beta_1$
$F_1=d$	$\frac{\alpha}{2}\sum_{i=1,3}\rho_i^2+\frac{\beta_1}{4}\sum_{i=1,3}\rho_i^4+\frac{\beta_2}{4}\sum_{i=1,3}\rho_i^4\cos 4\psi_i$ $+\frac{\beta_3}{4}(\rho_1^2\rho_2^2+\rho_1^2\rho_3^2+\rho_2^2\rho_3^2)$ $+\frac{\beta_4}{2}(\rho_1^2\rho_2^2\sin 2\psi_1\sin 2\psi_2+\rho_1^2\rho_3^2\sin 2\psi_1\sin 2\psi_3$ $+\rho_2^2\rho_3^2\sin 2\psi_2\sin 2\psi_3)$ $+\frac{\beta_5}{2}[\rho_1^2\rho_2^2(\sin 2\psi_1-\sin 2\psi_2)+\rho_2^2\rho_3^2(\sin 2\psi_2-\sin 2\psi_3)$ $+\rho_1^2\rho_3^2(\sin 2\psi_3-\sin 2\psi_1)]$ $[\eta_{2P+1}=\rho_{P+1}\cos\psi_{P+1}\ (P=0,1,2);$ $\eta_{2P}=\rho_P\sin\psi_P\ (P=1,2,3)]$	I $\rho_1^2=-\alpha/\beta_1+\beta_2,\rho_2=\rho_3=0,\psi_1=0$	$\beta_1>0,\beta_1+\beta_2>0,\beta_2<0$
		II $\rho_1^2=-\alpha/\beta_1-\beta_2,\rho_2=\rho_3=0,\psi_1=\frac{\pi}{4}$	$\beta_1>0,\beta_1-\beta_2>0,\beta_2>0$
		III $\rho_1^2=\rho_2^2=-\alpha/\Delta_1,\rho_3=0,\psi_1=-\psi_2=\frac{\pi}{4}$	$\Delta_1>0,2\beta_2+\beta_4-\beta_5>0,\beta_1-\beta_2>0$
		IV $\rho_1^2=\rho_2^2=\rho_3^2=-\alpha/\Delta_2,\ \psi_1=\psi_2=\psi_3=\frac{\pi}{4}$	$\beta_1>0,\beta_2-\beta_4>0,\beta_1-\beta_2>0,\Delta_2>0$; $\Delta_2(\beta_i)=\beta_1-\beta_2+2\beta_3+2\beta_4>0$
		V, VI $\rho_1^2=\rho_2^2=\rho_3^2=-\alpha/\Delta_3$ with $\psi_1=\psi_2=\psi_3=\frac{\pi}{2}$ or $\psi_1=\psi_2=\psi_3=0$	$\beta_1>0,\beta_1+\beta_2>\lvert\beta_3\rvert$; $\Delta_3>0,\Delta_4+8\epsilon\beta_1^2\beta_4\beta_5>0$; $\epsilon=+1$ or $\epsilon=-1$
		VII $\rho_1^2=-\alpha/\Delta_7,\rho_2^2=\rho_3^2=-\alpha/\Delta_8,\psi_1=0,\psi_2=\frac{\pi}{4},\psi_3=3\frac{\pi}{4}$	$\beta_1+\beta_2-\beta_3+\beta_5>0\}\Delta_7>0,\Delta_8>0,\Delta_{10}>0$
		VIII $\rho_1^2=-\alpha/\Delta_5,\rho_2^2=\rho_3^2=-\alpha/\Delta_6,\psi_1=0,\psi_2=3\frac{\pi}{4}\psi_3=\frac{\pi}{4}$	$\beta_2<0,\beta_1+\beta_2>0\}\Delta_5>0,\Delta_6>0,\Delta_9>0$

$\Delta_1=\beta_1-\beta_2+\beta_3-\beta_4+2\beta_5$; $\Delta_2=\beta_1-\beta_2+2(\beta_3+\beta_4)$; $\Delta_3=\beta_1+\beta_2+2\beta_3$; $\Delta_4=4\beta_1^2(3\beta_4^2-8\beta_1^2-4\beta_1\beta_2)+2\beta_4^2(2\beta_1\beta_2+\beta_1\beta_4+\beta_2\beta_4)+\beta_5^2(2\beta_4^2+3\beta_1\beta_4-6\beta_1^2)$;

$\Delta_5=\frac{(\beta_1+\beta_2)(\beta_1-\beta_2+\beta_3-\beta_4+2\beta_5)-2(\beta_3-\beta_5)^2}{\beta_1-\beta_2-\beta_3-\beta_4}$; $\Delta_6=\frac{2(\beta_3-\beta_5)\Delta_5}{\Delta_5+(\beta_1+\beta_2)}$; $\Delta_7=\Delta_5(\beta_1,\beta_2,\beta_3,\beta_4,-\beta_5)$;

$\Delta_8=\Delta_6(\beta_1,\beta_2,\beta_3,\beta_4,-\beta_5)$; $\Delta_9=(2\beta_1+\beta_4-2\beta_5)\rho_2^2+2\beta_5\rho_1^2\rho_2^2$; $\Delta_{10}=(2\beta_1+\beta_4+2\beta_5)\rho_2^2-2\beta_5\rho_1^2\rho_2^2$

3. The orthorhombic symmetries reported for Ni-Cl(mm2,m'm2'), Ni-Br(m'm2'), Co-Br(m'm2'), and Cu-Cl(m'm'2) can be induced by four different one-dimensional IC's ($\tau_1 \rightarrow \tau_4$) of the $Pca2_11'$ group, at the center of the primitive orthorhombic Brillouin zone. On the other hand, only the antiferromagnetic group $mm2$ could be connected to another IC in Table II, namely the same $\tau_1(X)$ IC of the $F\bar{4}3c\,1'$ group. This reasonably allows us to choose $Pca\,2_11'$ as corresponding to the parent phase for this third subclass of magnetic boracites. As it will be shown below, such a choice is consistent with the weak-ferromagnetic character of the low-temperature phases in Ni-Cl or Ni-Br, as well as with the magnetoelectric anomalies evidenced in these compounds.

Having identified the symmetries of the irreducible degrees of freedom associated with the phase transitions in the three groups of boracites listed in Table I, we are now able to discuss the coupling of the order-parameter to secondary physical quantities involved in the transitions.

C. General form of the Landau expansion and coupling to the order parameter

In addition to the order-parameter expansion, the Landau free energy which accounts for the phenomenological properties of a transition, contains terms relative to the macroscopic quantities (x_j) which couple to the order-parameter components (η_i). Two main situations are usually distinguished,[77] on the basis of the relative symmetries of the (η_i) and the (x_j): (i) When the (x_j) belong to the same irreducible degree of freedom as the order parameter, the corresponding transition is labeled as *proper*[78,79] if the (x_j) identify the order parameter, and *pseudoproper* if the (x_j) are bilinearly coupled to the order parameter. (ii) If the sets (x_j) and (η_i) belong to different irreducible degrees of freedom, the considered transition is an *improper* one.[78,79] For improper and pseudoproper transitions the Landau free energy splits into three kinds of terms:

$$F(\alpha,\eta_i,x_j,\beta_k,\lambda_l,\delta_m) = F_1(\alpha,\eta_i,\beta_k)+F_2(x_j,\lambda_l)+F_3(\eta_i,x_j,\delta_m)\,, \quad (1)$$

representing, respectively, the order-parameter expansion (F_1), the energy associated with the macroscopic tensors x_j (F_2), and the mixed invariants relative to the preceding quantities (F_3). $\alpha=a(T-T_c)$ is the temperature-dependent coefficient of the quadratic order-parameter invariant, whereas β_k, λ_l, and δ_m are temperature independent coefficients of the other terms constituting the Landau free energy.

The concepts of improper and pseudoproper transitions have been, up to now, almost restricted to structural transitions (i.e., to ferroelectrics and ferroelastics). However, they can also apply to a number of magnetic transitions, in particular to those transitions where the magnetization results from an antiferromagnetic ordering with an incomplete compensation of the magnetic moments. Although different denominations were introduced for such situations (i.e., weak ferromagnetism, canted and latent antiferromagnetism, ferrimagnetism), they can be treated, in the framework of the Landau theory, as improper or pseudoproper ferromagnetic transitions. Indeed, this is what was actually done, though using a different formalism (see Sec. VI), in the phenomenological theories of Dzialoshinskii[46,47,80] and Nikitin.[81]

In the boracite compounds under consideration, a number of experimental facts strongly suggest that the primary order parameter of the whole set of magnetic transitions is an antiferromagnetic ordering of the magnetic moments. These facts are (i) the typical negative asymptotic Curie-Weiss temperature determined from the magnetic susceptibilities;[3] (ii) the weak values of the measured magnetization (see the values in Table I) compared to the hypothetical values corresponding to the sum of the effective moments, deduced from susceptibility measurements;[8] (iii) the neutron-diffraction evidence of antiferromagnetic sublattices in Ni-I (Refs. 82 and 83) and Co-I;[84] (iv) the identification of antiferromagnetic intermediate phases in Ni-Cl (Ref. 32) and Co-I.[84]

The spontaneous magnetization **M**, polarization **P**, and strain e_{ij} are thus in our model, secondary order parameters resulting from an improper or pseudoproper coupling to the (primary) antiferromagnetic ordering. Such an interpretation is consistent with that given for Ni-I boracite in Refs. 40–44 and Ref. 85, but disagrees with the proposal of Newnham *et al.*[86] who claimed the spontaneous polarization to be the primary order parameter in this material. It is worth mentioning that symmetry arguments forbid the existence of a transition from a paramagnetic-paraelectric phase to a ferromagnetic-ferroelectric phase, in which the magnetization is induced by the polarization, considered as the primary order parameter.[87]

To complete the construction of the Landau free energy for each subclass of magnetic boracites, we must determine the F_2 and F_3 terms in (1). Various authors[79,88] have emphasized that it is sufficient to expand the F_2 contribution up to the quadratic terms only. Thus F_2 will coincide with the sum of the magnetic, dielectric and elastic energies, limited to the terms depending on the spontaneous components of **M**, **P**, and e_{ij}. The coupling of the preceding components (x_j) with the (η_j) will be represented in F_3 by terms of the form $\phi(\eta_i)\psi(x_j)$, where ϕ and ψ have identical symmetries and where $\phi(\eta_i)=0$ in the high-symmetry phase. In this respect, it has been established,[79] that the lowest degree invariants in F_3 are necessarily *linear* functions of the x_j components. Whenever these components below to several IC's (τ_m) of the paramagnetic group, each IC will give rise to an invariant of the form $\delta_m \sum_j x_j\phi_j(\eta_i)$, where the ϕ_j are homogeneous polynomials of degree q obtained by projecting the IC inducing the transition upon τ_m. In the vicinity of the transition point it is sufficient to consider the set of ϕ_j functions having the *smallest* degree $q=\nu$. The degree ν has been called the faintness index[88] relative to the ferroic property (i.e., ferromagnetic, ferroelectric, ferroelastic).

The F_2 and F_3 contributions have been worked out for the relevant IC's of the $F43c\,1'$, $R3c\,1'$, and $Pca\,2_11'$ Shubnikov groups. They are given, respectively, in Tables IV, VI,and VII. We shall now discuss the physical consequences of such contributions in relationship with the ob-

served anomalies in each of the corresponding subclass of boracites.

III. APPLICATION TO Ni-I BORACITE

Table IV contains the mixed invariants which couple to the six-dimensional order parameter, respectively: the spontaneous magnetization components (M_x,M_y,M_z), the spontaneous polarization components (P_x,P_y,P_z), and the spontaneous strain components (e_1–e_6). The couplings between the M_u,P_u ($u=x,y,z$) and e_i ($i=1,6$) have been also worked out, in order to account for the magnetoelectric, piezoelectric, and magnetoelastic effects.

A. Magnetic properties

Let us first discuss the magnetic properties of Ni-I. Expression for the equilibrium values of the spontaneous magnetization components at zero magnetic field, are found by minimizing the Landau free energy $F=F_1+F_2+F_3$ with respect to the ρ_i, ψ_i ($i=1,2,3$), and M_u ($u=x,y,z$). However, as taking into account the coupling terms F_M, F_{ME}, and $F_{\rho\mathrm{ME}}$ is tantamount to introducing at least six-degree terms in the ρ_i, we can assume in a first approximation that the equilibrium values for the order-parameter components in the low-temperature phase are those obtained by the sole minimization of F_1, namely (see Table III)

$$\rho_1^e=\left[-\frac{\alpha}{\Delta_7}\right]^{1/2},\quad \rho_2^e=\rho_3^3=\left[-\frac{\alpha}{\Delta_8}\right]^{1/2},$$
$$\psi_1^e=0,\quad \psi_2^e=\frac{\pi}{4},\quad \psi_3^3=3\frac{\pi}{4}\ . \tag{2}$$

Thus for $T<T_c$, the ρ_i have the usual $(T_c-T)^{1/2}$ variation, a result which is to be compared with the temperature variation of the antiferromagnetic sublattice magnetization as determined by von Wartburg[83] from neutron intensities. The curve shown in Ref. 83 indeed corresponds to the expected variation. It also reveals a clear-cut second-order characteristic for the $T_c=61.5$ K transition. Accordingly, in the vicinity of T_c, it is sufficient to retain only the lower-degree coupling terms in $F_M(\mathbf{H}=\mathbf{0})$, in order to find the equilibrium values for the M_u. One attains

$$M_u=\chi_0^M\rho_1^e\rho_2^e\rho_3^e f_u(\delta_1,\delta_2,\psi_1^e,\psi_2^e,\psi_3^e)\ ; \tag{3}$$

the f_u functions ($u=x,y,z$) are defined in Table V(a). Introducing in (3) the equilibrium values (2) yields

TABLE IV. Coupling terms for the $F\bar{4}3c\,1'\rightarrow Cc'$ transition in Ni-I boracite, between the six-component order parameter (ρ_i,ψ_i) ($i=1$–3) and the (a) magnetization, (b) polarization, and (c) strain components, respectively. F_M, F_E, and F_S also contain the relevant magnetic, dielectric and elastic energies. (d) Magnetoelectric F_{ME}, magnetoelastic F_{MS}, and piezoelectric F_{ES} coupling terms. $F_{\rho\mathrm{ME}}$ relates all ρ_i M_u, and P_u components ($u=x,y,z$).

(a)

$$\begin{aligned}F_M=&\delta_1\rho_1\rho_2\rho_3(M_1\cos\psi_1\cos\psi_2\cos\psi_3+M_2\sin\psi_1\cos\psi_2\sin\psi_3\\&-M_3\cos\psi_1\sin\psi_2\sin\psi_3-M_4\sin\psi_1\sin\psi_2\cos\psi_3)\\&+\delta_2\rho_1\rho_2\rho_3(-M_1\sin\psi_1\sin\psi_2\sin\psi_3-M_2\cos\psi_1\sin\psi_2\cos\psi_3\\&+M_3\sin\psi_1\cos\psi_2\cos\psi_3+M_4\cos\psi_1\cos\psi_2\sin\psi_3)\\&+\frac{1}{2\chi_0^M}(M_x^2+M_y^2+M_z^2)+\frac{\mu_1}{2}(M_x^2\rho_2^2+M_y^2\rho_1^2+M_z^2\rho_3^2)\\&+\frac{\mu_2}{2}[M_x^2(\rho_1^2+\rho_3^2)+M_y^2(\rho_2^2+\rho_3^2)+M_z^2(\rho_1^2+\rho_2^2)]\\&+\frac{\mu_3}{2}(M_x^2+M_y^2+M_z^2(\rho_1^2+\rho_2^2+\rho_3^2)-\mathbf{H}\cdot\mathbf{M}\end{aligned}$$

$(M_1=M_x+M_y+M_z, M_2=M_x-M_y-M_z, M_3=M_x-M_y+M_z,$
$M_4=M_x+M_y-M_z)$

(b)

$$\begin{aligned}F_E=&\delta_1(P_x\rho_1^2\cos2\psi_1+P_y\rho_2^2\cos2\psi_2)+\delta_2(P_x\rho_3^2\cos2\psi_3+P_z\rho_2^2\cos2\psi_2)\\&+\delta_3(P_y\rho_3^2\cos2\psi_3+P_z\rho_1^2\cos2\psi_1)+\delta_4(P_x\rho_2^2\cos2\psi_2+P_y\rho_1^2\cos2\psi_1\\&+P_z\rho_3^2\cos2\psi_3)\\&+\frac{1}{2\chi_0^E}(P_x^2+P_y^2+P_z^2)+\frac{\mu_1}{2}(P_x^2\rho_2^2+P_y^2\rho_1^2+P_z^2\rho_3^2)\\&+\frac{\mu_2}{2}[P_x^2(\rho_1^2+\rho_3^2)+P_y^2(\rho_2^2+\rho_3^2)+P_z^2(\rho_1^2+\rho_2^2)]-\mathbf{E}\cdot\mathbf{P}\end{aligned}$$

(c)

$$\begin{aligned}F_S=&\delta_1(e_4\rho_1^2\cos2\psi_1+e_5\rho_2^2\cos2\psi_2)\\&+\delta_2(e_4\rho_3^2\cos2\psi_3+e_6\rho_2^2\cos2\psi_2)\\&+\delta_3(e_5\rho_3^2\cos2\psi_3+e_6\rho_1^2\cos2\psi_1)\\&+\delta_4[e_1(\rho_1^2\sin2\psi_1-\rho_3^2\sin2\psi_3)\\&+e_2(\rho_3^2\sin2\psi_3-\rho_2^2\sin2\psi_2)\\&+e_3(\rho_2^2\sin2\psi_2-\rho_1^2\sin2\psi_1)]\\&+\delta_5(e_4\rho_2^2\cos2\psi_2+e_5\rho_1^2\cos2\psi_1\\&+e_6\rho_3^2\cos2\psi_3)+\delta_6(e_1\rho_2^2+e_2\rho_1^2+e_3\rho_3^2)\\&+\delta_7[e_1(\rho_1^2+\rho_3^2)+e_2(\rho_2^2+\rho_3^2)+e_3(\rho_1^2+\rho_2^2)]\\&+\tfrac{1}{2}C_{11}^0(e_1^2+e_2^2+e_3^2)+C_{12}^0(e_1e_2+e_1e_3+e_2e_3)\\&+\tfrac{1}{2}C_{44}^0(e_4^2+e_5^2+e_6^2)-\sum_{i,j}\sigma_{ij}e_{ij}\end{aligned}$$

(d)

$$\begin{aligned}F_{\mathrm{ME}}=&\alpha_0(P_xM_yM_z+P_yM_xM_z+P_zM_xM_y)\\F_{\mathrm{MS}}=&\alpha_1(e_4M_yM_z+e_5M_xM_z+e_6M_xM_y)\\&+\alpha_2e_1(M_y^2+M_z^2)+e_2(M_x^2+M_z^2)+E_3(M_x^2+M_y^2)\\&+\alpha_3(e_1M_x^2+e_2M_y^2+e_3M_z^2)\\F_{\mathrm{ES}}=&\gamma(P_xe_4-P_ye_5+P_ze_6)\\F_{\rho\mathrm{ME}}=&\gamma(M_xM_yP_z+M_yM_zP_x+M_xM_zP_y)(\rho_1^2+\rho_2^2+\rho_3^2)\end{aligned}$$

TABLE V. Ni-I boracite: (a) functions expressing the ψ_i dependence of the magnetization components M_u ($u=x,y,z$) in the monoclinic phase. (b) Linear relationships between the components of the dielectric susceptibility tensor. (c) Magnetoelectric equations relating the magnetization and polarization components, under application of an electric or magnetic field.

(a)

$$f_x=\delta_1(\cos\psi_1\cos\psi_2\cos\psi_3+\sin\psi_1\cos\psi_2\sin\psi_3-\cos\psi_1\sin\psi_2\sin\psi_3-\sin\psi_1\sin\psi_2\cos\psi_3)$$
$$+\delta_2(-\sin\psi_1\sin\psi_2\sin\psi_3-\cos\psi_1\sin\psi_2\cos\psi_3+\sin\psi_1\cos\psi_2\cos\psi_3+\cos\psi_1\cos\psi_2\sin\psi_3)$$
$$f_y=\delta_1(\cos\psi_1\cos\psi_2\cos\psi_3-\sin\psi_1\cos\psi_2\sin\psi_3+\cos\psi_1\sin\psi_2\sin\psi_3-\sin\psi_1\sin\psi_2\cos\psi_3)$$
$$+\delta_2(-\sin\psi_1\sin\psi_2\sin\psi_3+\cos\psi_1\sin\psi_2\cos\psi_3-\sin\psi_1\cos\psi_2\cos\psi_3+\cos\psi_1\cos\psi_2\sin\psi_3)$$
$$f_z=\delta_1(\cos\psi_1\cos\psi_2\cos\psi_3-\sin\psi_1\cos\psi_2\sin\psi_3-\cos\psi_1\sin\psi_2\sin\psi_3+\sin\psi_1\sin\psi_2\cos\psi_3)$$
$$+\delta_2(-\sin\psi_1\sin\psi_2\sin\psi_3+\cos\psi_1\sin\psi_2\cos\psi_3+\sin\psi_1\cos\psi_2\cos\psi_3-\cos\psi_1\cos\psi_2\sin\psi_3)$$

(b)

$$\chi^E_{11}=\frac{\chi^E_0}{\pi(\delta_1)}\left[1+\frac{2\delta_1}{\Delta}(\delta_3\chi^E_{13}+\delta_4\chi^E_{12})\right],\quad \chi^E_{22}=\frac{\chi^E_0}{\pi(\delta_4)}\left[1+\frac{2\delta_4}{\Delta}(\delta_1\chi^E_{12}+\delta_3\chi^E_{23})\right]$$
$$\chi^E_{33}=\frac{\chi^E_0}{\pi(\delta_4)}\left[1+\frac{2\delta_4}{\Delta}(\delta_1\chi^E_{12}+\delta_3\chi^E_{23})\right],\quad \chi^E_{12}=\frac{2\chi^E_0\delta_1}{\Delta\pi(\delta_1)}(\delta_3\chi^E_{23}+\delta_4\chi^E_{22})$$
$$\chi^E_{13}=\frac{2\chi^E_0\delta_4}{\Delta\pi(\delta_1)}(\delta_3\chi^E_{33}+\delta_4\chi^E_{23}),\quad \chi^E_{23}=\frac{2\chi^E_0\delta_3}{\Delta\pi(\delta_3)}(\delta_1\chi^E_{12}+\delta_4\chi^E_{23})$$
$$\pi(\delta)=1/1-2x^E_0\frac{\delta^2}{\Delta},\quad \Delta=\beta_1+\beta_2+2(\beta_3+\beta_5)\frac{\Delta_7}{\Delta_8}$$

(c)

$$P_x=-\chi^E_0[A(\rho_i)M_yM_z+\delta_1\rho_1^2-E_x],\quad P_y=-\chi^M_0[A(\rho_i)M_xM_z+\delta_4\rho_1^2-E_y]$$
$$P_z=-\chi^E_0[A(\rho_i)M_xM_y+\delta_3\rho_1^2-E_z],\quad M_x=-\chi^M_0[A(\rho_i)(P_zM_y+P_yM_z)-(\delta_2-\delta_1)\rho_1\rho_2\rho_3-H_x]$$
$$M_y=-\chi^M_0[A(\rho_i)(P_xM_z+P_zM_x)-H_y],\quad M_z=-\chi^M_0[A(\rho_i)(P_yM_x+P_xM_y)-(\delta_1+\delta_2)\rho_1\rho_2\rho_3-H_z]$$
$$A(\rho_i)=\alpha_0+\gamma(\rho_1^2+\rho_2^2+\rho_3^2)$$

$$M_z(E_y)=\alpha_0\chi^E_0(\chi^M_0)^2(\delta_1-\delta_2)\rho_1\rho_2\rho_3(E_y-\delta_4\rho_1^2)$$
$$M_y(E_z)=\alpha_0\chi^E_0(\chi^M_0)^2(\delta_1-\delta_2)\rho_1\rho_2\rho_3[E_z-(\delta_1+\delta_2+\delta_3)\rho_1^2]$$
$$M_y(E_x)=\alpha_0\chi^E_0(\chi^M_0)^2\rho_1\rho_2\rho_3[-(\delta_1+\delta_2)E_x+(\delta_1^2+\delta_1\delta_2-\delta_1\delta_3+\delta_2\delta_3)\rho_1^2]$$
$$M_x(E_y)=\alpha_0\chi^E_0(\chi^M_0)^2\rho_1\rho_2\rho_3(-E_y+\delta_4\rho_1^2)$$

$$M_x=(\delta_1+\delta_2)\Delta(T),\quad M_y=0,\quad M_z=(\delta_1-\delta_2)\Delta(T)$$

where $\Delta(T)=\chi^M_0\Delta_7^{-1/2}\Delta_8^{-1}[a(T_c-T)]^{3/2}$. The zero value obtained for the M_y component indicates that the spontaneous magnetization which lies below T_c in the $\sigma_{\bar{x}y}$ plane ($\sigma_{\bar{x}z}$ when referring to the F cubic cell), is perpendicular to the $[01\bar{1}]$ direction. However, such a property is valid only in the considered approximation which assumes the equilibrium values (2) for the order-parameter components, i.e., in the vicinity of T_c. Let us also note that the critical exponent $\frac{3}{2}$ found for the temperature dependence of M_x and M_z, which corresponds to a faintness index $\nu=3$, was pointed out by Dzialoshinskii and Man'ko[47] as characterizing latent antiferromagnetic materials (see Sec. VI).

Far from T_c, for large values of the ρ_i, one cannot neglect the higher degree terms in F_M. Expressions for the components M_x and M_z are

$$M_x=\frac{(\delta_1+\delta_2)\rho_1^e\rho_2^e\rho_3^e}{(\chi^M_0)^{-1}+g(\mu_i,\rho_i^e)},\quad M_z=\frac{(\delta_1-\delta_2)\rho_1^e\rho_2^e\rho_3^e}{(\chi^M_0)^{-1}+g(\mu_i,\rho_i^e)},$$

with $g(\mu_i,\rho_i^e)=\mu_1\rho_2^{e^2}+\mu_2(\rho_1^{e^2}+\rho_3^{e^2})+\mu_3(\rho_1^{e^2}+\rho_2^{e^2}+\rho_3^{e^2})$. Thus, M_x and M_z vary asymptotically as $(T_c-T)^{1/2}$. The curve $M_u(T)$ ($u=x,y$) is drawn schematically in Figs. 5(a). One can find some resemblance with an unpublished experimental curve for the sublattice magnetization, measured by Fischer[89] from neutron intensities, and reproduced in Fig. 5(b). On this curve, however, the $(T_c-T)^{3/2}$ regime appears to be limited to a narrow region close to T_c where it is difficult to distinguish from the diffuse behavior commonly found in the critical region for continuous transitions.

Similarly the schematic character of the magnetization

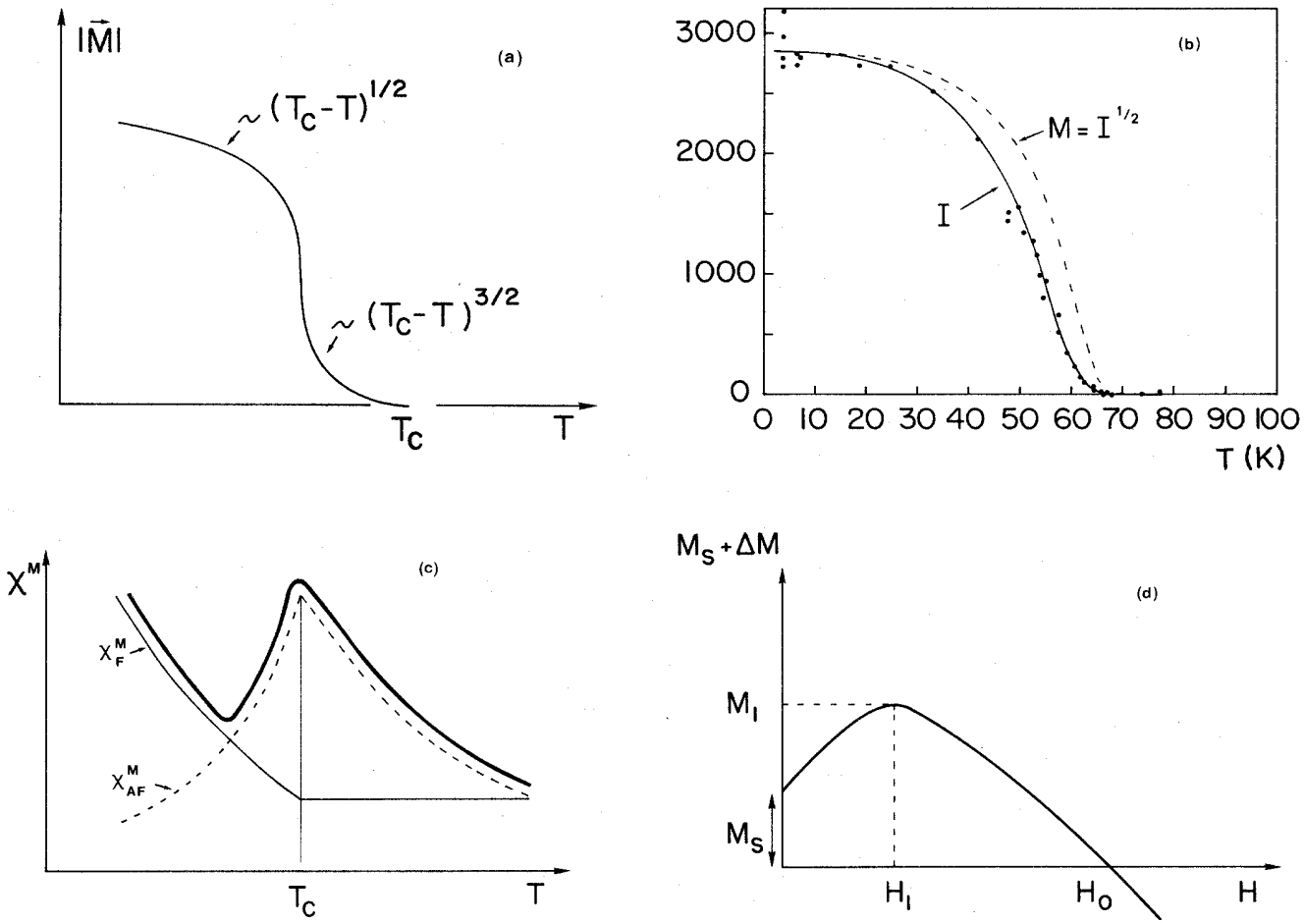

FIG. 5. Ni-I boracite. Temperature dependence of the magnetization: (a) theoretical curve; (b) experimental curve deduced from the intensity I of the magnetic (111) neutron reflection (Ref. 89). (c) Temperature dependence of the total magnetic susceptibility $\chi^M=\chi^M_{AF}+\chi^M_F$. (d) Predicted variation for the magnetic field dependence of the magnetization for certain directions of **H**.

curve $M_x(T)$ found by Baturov *et al.*[34] by the Faraday method, does not allow comparison with the theoretical variation shown on Fig. 5(a) in the vicinity of T_c. However, the curve given in Ref. 34 displays a remarkable feature below 50 K, namely a sharp drop of about one-half of its maximal value. Such an unusual behavior may be attributed to a rotation of the magnetization vector in the m' plane, with a decreasing of the M_x projection. It implies however a rather large rotation of **M**, while the spontaneous Faraday rotation versus temperature perpendicular to the (001) cut face does not show any decrease along z at low temperature.[14] The decrease of $M_x(T)$ may also be due to the depoling of the sample occurring on cooling down which, in the absence of an electric field, brings along a depolarization of the resultant of the magnetic moment. Such an effect was already observed in some boracites.[90]

The magnetic susceptibility χ^M should represent the dual nature of the transition in Ni-I as assumed in our model. Thus χ^M must be written as the sum of two contributions: $\chi^M=\chi^M_{AF}+\chi^M_F$, where χ^M_{AF} accounts for the antiferromagnetic ordering, and has the usual temperature variation for the susceptibility in antiferromagnetic compounds [dotted line on Fig. 5(c)]. Obtained for χ^M_F is

$$\chi^M_F=\lim_{H\to 0}\left[\frac{\partial M}{\partial H}\right]_{\rho_i=0}\sim\frac{\chi^M_0}{1-\Delta(\delta_i,\beta_i)\chi^M_0\rho_1\rho_2\rho_3}$$

$$[\Delta(\delta_i,\beta_i)>0]\,,$$

which accounts for the improper ferromagnetic character of the transition [solid line on Fig. 5(c)]. The theoretical variation shown on Fig. 5(c) for the total susceptibility $\chi^M(T)$ is partly verified by the experimental curves given in Refs. 4 and 91. Thus, the susceptibility measured on powders by Ascher *et al.*[4] shows a sharp decrease on cooling to about 30 K, where it starts increasing again down to 4 K. The same nonmonotonic variation is found in the single-crystal measurement of Zheludev *et al.*[91] However, for $T\geq T_c$ the two experimental curves display features which are not observed on Fig. 5(c), namely (i) an upward jump at T_c which is found on cooling in Ref. 4, and on heating in Ref. 79. In our model such a jump can be ob-

tained only if we assume the transition to be first order. (ii) There is an increase[4] or a constant value[91] of $\chi^M(T)$ for $T > T_c$. Let us note that this latter contradiction between the experimental data confirms the nonintrinsic character[58,54] of the broad maximum at 120 K found in Ref. 4.

Finally, let us consider the magnetic field dependence of the magnetization in the low-temperature phase. This dependence was evidenced experimentally by an hysteresis loop of Faraday rotation along the [110] direction[92] and by magnetization curves $M_u(H)$ for $\mathbf{H}||[110]$ and $\mathbf{H}||[1\bar{1}1]$.[91] The hysteresis loop reveals a strong asymmetry of the rotation angle.[92] On the other hand, while for $\mathbf{H}||[110]$ the curve $M(H)$ increases linearly for large fields, it decreases for $\mathbf{H}||[1\bar{1}1]$ above 3 kOe and changes sign above 20 kOe.[92] This experimental behavior can be foreseen using the simplified one-component free energy:

$$F = F_0 + \frac{\alpha}{2}\eta^2 + \frac{\beta}{4}\eta^4 + \frac{1}{2\chi_0^M}M^2 + \delta\eta^3 M - MH \ ,$$

which, according to our model, contains a $\nu=3$ faintness index coupling term. From the equilibrium equations, one obtains

$$H = \frac{M}{\chi_0^M} + \delta\eta_{1,2}^3 \ ,$$

with (4)

$$\eta_{1,2} = -\frac{3\delta M}{2\beta} \pm \frac{(9\delta^2M^2 - 4\alpha\beta)^{1/2}}{2\beta} \ .$$

Thus the $M(H)$ curve intersects the $H=0$ axis at the two *asymmetric* values: $M_{1,2} = -\chi_0^M \delta\eta_{1,2}^3$. On the other hand, one can deduce from (4),

$$H(M) = AM - BM^3 \pm j(\beta,\delta,M,\alpha) \ , \tag{5}$$

with

$$A = (\chi_0^M)^{-1} + \frac{3\delta^2\alpha}{2\beta^2}, \quad B = \frac{27\delta^2}{4\beta^3} > 0$$

and

$$j(\beta,\delta,M,\alpha) = \left[\frac{9\delta^2M^2 - \alpha\beta}{2\beta^3}\right](9\delta^2M^2 - 4\alpha\beta)^{1/2} > 0 \ .$$

For small values of H (i.e., $H \ll 3$ kOe) a *linear* $M \simeq AM$ variation should be observed for any direction of H, while for large values of the H components parallel to the monoclinic plane $\sigma_{\bar{x}z}$ containing the spontaneous magnetization, the $M(H)$ curve should start decreasing for M_1 given by

$$A - 3BM_1^2 \pm \left[\frac{\partial j}{\partial M}\right]_{M=M_1} = 0 \ ,$$

and reverse sign for H_0 corresponding to $H_0 = -(\alpha/2\beta^2)(-4\alpha\beta)^{1/2}$ [Fig. 5(d)].

B. Dielectric and elastic properties

The dielectric properties of Ni-I in the vicinity of T_c clearly denote the improper character of the ferroelectric transition. In this respect the value of P_s at 4.5 K ($P_s \simeq 0.078$ μC/cm^2) (Ref. 14) is about two orders of magnitude smaller than the corresponding value for $Gd_2(MoO_4)_3$ (Ref. 93) which is the textbook example of an improper ferroelectric. Minimization of $F_1 + F_E$ ($E=0$) with respect to P_u ($u = x,y,z$) yields

$$P_x = -\frac{\delta_1\chi_0^E\rho_1^2}{1+\chi_0^E[\mu_1\rho_2^2 + \mu_2(\rho_1^2+\rho_3^2)]} \ ,$$

$$P_y = -\frac{\delta_4\chi_0^E\rho_1^2}{1+\chi_0^E[\mu_1\rho_1^2 + \mu_2(\rho_2^2+\rho_3^2)]} \ ,$$

and

$$P_z = -\frac{\delta_3\chi_0^E\rho_1^2}{1+\chi_0^E[\mu_1\rho_3^2 + \mu_2(\rho_1^2+\rho_2^2)]} \ .$$

Thus near below T_c (i.e., for $\mu_i\rho_j^2 \ll 1/\chi_0^E$) one should observe a linear temperature variation for the P_u:

$$P_u \simeq -\frac{\delta_i\chi_0^E a}{\Delta_7}(T_c - T) \ , \tag{6}$$

a behavior which corresponds to a faintness index $\nu=2$. At lower temperatures for larger values of the ρ_i, the temperature dependence of, for example P_x, should follow the law

$$P_x = \frac{A(T-T_c)}{1-B(T-T_c)}$$

with

$$A = \frac{\delta_1\chi_0^E a}{\Delta_7}$$

and

$$B = a\chi_0^E\left[\frac{\mu_1}{\Delta_8} + \mu_2\left[\frac{1}{\Delta_7} + \frac{1}{\Delta_8}\right]\right] .$$

The theoretical variation of $P_x(T)$ is shown on Fig. 6(a). In Fig. 6(b) the pyroelectric coefficient $p = dP_s/dT$ is represented and undergoes a jump at T_c corresponding to

$$\Delta p = \frac{\delta_1\chi_0^E a}{\Delta_7} \ .$$

p remains constant in the interval of velocity of the linear law (6), then decreases as

$$p = \frac{A}{[1-B(T-T_c)]^2} \ .$$

The experimental curves given in Ref. 14 for $P_s(T)$ and $p(T)$ are in substantial agreement with the preceding theoretical variations. However the comparison reveals that a linear variation for P_s can be assumed only in the close vicinity of T_c. Besides, the pyroelectric coefficient p, deduced from an independent pyroelectric measurement, shows a sharp peak at T_c. It may be attributed to the effect of fluctuations in the critical region, which have not been taken into account in our model. Indeed, fluctuations will determine a concave variation of P_s, rather

than the mean-field linear one.

Using the F_E ($E\neq 0$) terms given in Table IV allows us to obtain algebraic expressions for the six components χ_{ij}^E ($i,j=1,2,3$) of the dielectric susceptibility tensor. The linear equations providing the detailed form of the components are given in Table V(b). However, in order to obtain a qualitative behavior of the χ_{ij}^E as a function of temperature, one may use a one-component order-parameter model containing the characteristic $\eta^2 P$ coupling term introduced in our model. The simplified free energy,

$$F=F_0+\frac{\alpha}{2}\eta^2+\frac{\beta}{4}\eta^4+\frac{P^2}{2\chi_0^E}+\delta\eta^2 P-EP\ ,$$

yields

$$\chi^E=\lim_{E\to 0}\left[\frac{\partial P}{\partial E}\right]=\begin{cases}\chi_0^E & \text{in the paraelectric phase,}\\ \dfrac{\chi_0^E}{1-2(\chi_0^E/\beta)\delta^2} & \text{in the ferroelectric phase .}\end{cases}$$

Accordingly $\chi^E(T)$ undergoes an *upward* jump on cooling and remains constant on both sides of the transition [solid curve in Fig. 6(c)]. Such a temperature dependence is well illustrated by the experimental curves of Refs. 4 and 14 (in particular by the 1-MHz curve in Ref. 14), although one has to introduce, as usual, a linear dependence on temperature for the χ_0^E coefficient, in order to account for the thermal expansion [dotted curve in Fig. 6(c)].

The asymmetry of the dielectric hysteresis loop in the low-temperature phase, reported for Ni-I by Ascher *et al.*,[4] has been described by Chupis[75] as being an intrinsic property of the material. However, it is much more likely to be due to internal bias fields induced by growth defects as was frequently verified in most boracites[94] and in many other ferroelectrics.[95] Such a conclusion is also suggested by the experimental data of Miyashita and Murakami[92] who obtain either symmetric or asymmetric dielectric hysteresis loops, depending on the quality of the sample. From our model, asymmetric loops can only be obtained when taking into account coupling terms of unusually high degree between the spontaneous polarization and the order parameter.

Elastic data ascertaining the elastic properties of the transition in Ni-I are scarce. However, the anomaly observed for the C_{33} elastic constant[48,54] displays a typical drop as the temperature increases,[96] which is consistent with the improper character (with a $\nu=2$ faintness index) of the ferroelastic transition, as predicted by our model. On the other hand, the temperature dependence of the spontaneous birefringence Δn given in Ref. 14 should be proportional to some combination of the spontaneous strain tensor. It is worthwhile noting that Δn undergoes a discontinuity at T_c which contradicts the second-order character of the transition revealed by the other macroscopic quantities. Such a discontinuity may be due to parasitic birefringences[6] or to the optical tilting compensator method used.[97]

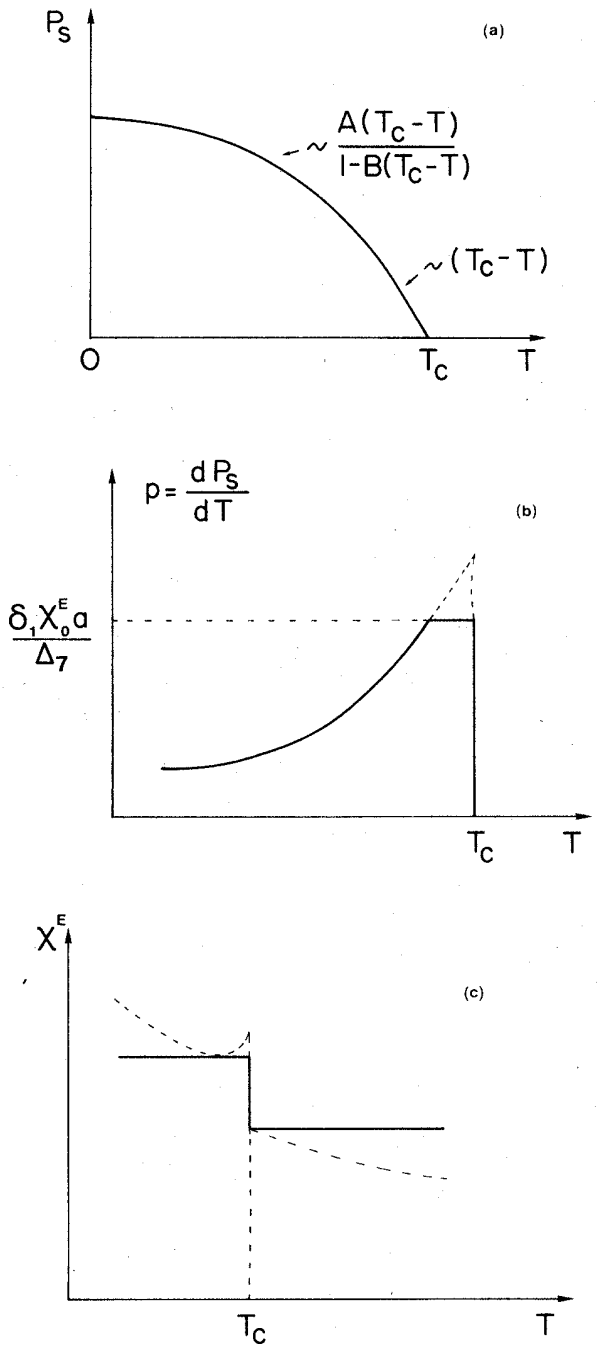

FIG. 6. Ni-I boracite. Theoretical curves for the temperature dependence of (a) the spontaneous polarization, (b) the pyroelectric coefficient, (c) the dielectric susceptibility.

C. Magnetoelectric properties

The straight coupling between magnetic and electric properties in Ni-I boracite below T_c is one of the most distinctive features of this material. It was evidenced ex-

perimentally by the switching of electric and magnetic domains under conjugated fields[4,6] and by a set of measurements which clearly show a spontaneous magnetoelectric effect.[4,6,13,98] In our model such effects are accounted by the coupling terms denoted F_{ME} and $F_{\rho\mathrm{ME}}$ in Table IV(d). Thus minimization with respect to P_z of the free energy $F=F_1+F_e(E\neq 0)+F_{\mathrm{ME}}$ yields the equation of state

$$\frac{P_z}{\chi_0^E}-E_z\simeq-\alpha_0(M_s^{\perp})^2\sin\theta\cos\theta\ , \tag{7}$$

where the spontaneous magnetization $M_s^{\perp}$ is located in the xy plane, θ is the angle between $M_s^{\perp}$ and the x axis [Fig. 7(a)]. From (7) one can see that a change of sign of the polarization under application of a suitable electric field ($E_z\rightarrow -E_z$, $P_z\rightarrow -P_z$) should result in a 90° rotation of $M_s^{\perp}$ in the xy plane ($\theta\rightarrow\theta+\pi/2$). This effect was obtained by Ascher *et al.*[4] by application of a ~ 5 kV/cm field at 56 K. The inverse effect, i.e., the reversal of P_z when an external magnetic field is applied perpendicular to the magnetization, evidenced by the same authors near T_c,[4,6] is expressed by the equation

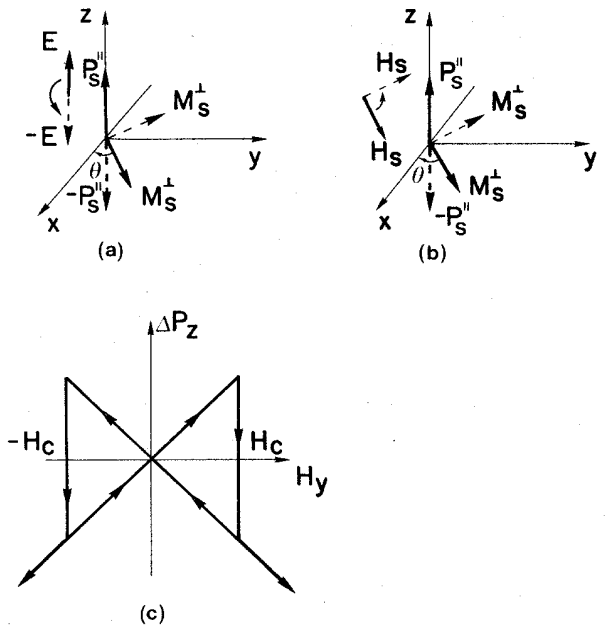

FIG. 7. Magnetoelectric properties of Ni-I boracite. (a) Rotation of the spontaneous magnetization component lying in the xy plane ($M_s^{\perp}$) when the polarization parallel to z changes sign under suitably applied electric field **E**. (b) Reversal of the polarization $P_s^{\parallel}$ when $M_s^{\perp}$ is turned in the xy plane under applied magnetic field $\mathbf{H}_s$. (c) Butterfly loop showing the dependence of the induced polarization ΔP_z under application of a magnetic field H_y.

$$[(\chi_0^M)^{-1}M_s^{\perp}-H_y]\sin\theta\simeq-\alpha_0 M_s^{\perp}P_z\cos\theta\ , \tag{8}$$

obtained by minimization of $F=F_1+F_M+F_{\mathrm{ME}}$ with respect to M_y. Here, one can see [Fig. 7(b)] that when turning the magnetization by 90° from the initial position $\theta=\pi/4$, under application of the corresponding magnetic fields ($\theta\rightarrow\theta+\pi/2$), one has to reverse the sign of P_z for Eq. (8) to remain unchanged. Equations providing the general relationships between the polarization and magnetization components, are given in Table V(c).

Introducing in (7) the equilibrium values for $M_x=M_s^{\perp}\cos\theta$ and $M_y=M_s^{\perp}\sin\theta$, one attains in the absence of applied electric field,

$$\Delta P_z\simeq\chi_0^E\alpha_0\frac{\delta_1+\delta_2}{(\chi_0^M)^{-2}}\rho_1\rho_2\rho_3 H_y\ , \tag{9}$$

where ΔP_z is the variation of polarization induced by application of a magnetic field. The dependence of ΔP_z as a function of H_y at given temperature $T<T_c$ is shown on Fig. 7(c). Starting from a negative value of H_y, one should observe a linear increase of ΔP_z with increasing H_y up to some coercive field H_y^c where the initial value of the ρ_i (i.e., the antiferromagnetic sublattice magnetization) becomes unstable and reverses sign ($\rho_i\rightarrow-\rho_i$), the corresponding value of ΔP_z falling abruptly to $-\Delta P_z$. Such a typical magnetoelectric butterfly loop was reported for Ni-I boracite in Refs. 4 and 6, for $\mathbf{H}\|[110]$. As can be deduced from the equations given in Table V(c), a similar loop should also be observed for $\mathbf{P}\|[100]$ and $\mathbf{H}\|[011]$. By contrast, it should differ for $\mathbf{P}\|[010]$ and $\mathbf{H}\|[101]$ as at zero magnetic field one should measure a nonvanishing spontaneous polarization (i.e., the loop should not be centered at the origin of the axes). It can be pointed out that the vanishing of P_z at zero magnetic field in the magnetoelectric hysteresis loop measured in Ref. 4, confirms indirectly the prediction deduced from our model, of a spontaneous magnetization $M_s^{\perp}$ perpendicular to the y axis. Let us also stress that the order-parameter dependence $\Delta P_z(\rho_i)$, expressed by Eq. (9), is corroborated by the optically determined switching-field—versus—temperature curve $H_c(T)$ given in Ref. 4. This curve shows an increase of the critical coercive field as the temperature is lowered (i.e., as ρ_i increases) with $H_c(T_c)=0$.

From Eq. (9) one can deduce the magnetoelectric coefficient

$$\alpha_{zy}=\left[\frac{\Delta P_z}{H_y}\right]_{\substack{\mathbf{E}\equiv 0\\ H_x=H_z=0}}\ ,$$
$$\alpha_{zy}\simeq\frac{\chi_0^E\alpha_0}{(\chi_0^M)^{-2}}(\delta_1+\delta_2)\rho_1\rho_2\rho_3\ . \tag{10}$$

Replacing the ρ_i by their equilibrium values (see Table III), one obtains $\alpha_{zy}=0$ for $T>T_c$ and $\alpha_{zy}\simeq A(T_c-T)^{3/2}$ for $T<T_c$ with

$$A=\frac{\chi_0^E\alpha_0(\delta_1+\delta_2)}{(\chi_0^M)^{-2}\Delta_7^{1/2}\Delta_8} .$$

The experimental curve found by Ascher *et al.*[4] for $\alpha(T)=\Delta P_z/H_{xy}$ [Fig. 7(d)] displays two features which are not accounted for by Eq. (10), namely a two-step regime as the temperature is lowered, and a negative peak in the close vicinity of T_c. The almost linear increasing of $\alpha(T)$ observed in Ref. 4 below 55 K may be connected with the asymptotic value reached by the sublattice magnetization (i.e., the ρ_i) in this interval.[83] In our calculation it could be accounted for by considering the higher-degree mixed coupling term, denoted $F_{\rho\mathrm{ME}}$ in Table IV. On the other hand, the sign reversal of α near T_c may be interpreted by the fact that the magnetization of a few percent of the sample assumes the direction of the applied field only close to the Curie point, resulting in a change of polarization—due to the 180° reversal of $P_s^{\parallel}$—opposite to the magnetoelectric effect. This latter explanation is supported by the observation that the negative peak becomes smaller when applying a strong magnetic field bias.[6]

The consistency of the preceding arguments can be checked by examining the experimental data obtained by Baturov *et al.*[13,98] who measured the reverse magnetoelectric effect, i.e., the magnetization component M_y induced by an applied electric field. From Table V(c), one can deduce the equations expressing the electric field dependence of the magnetization components. In particular, one has

$$\Delta M_y\simeq\chi_0^E\alpha_0\frac{\delta_1+\delta_2}{(\chi_0^M)^{-2}}\rho_1\rho_2\rho_3E_z . \tag{11}$$

A linear dependence $\Delta M_y=f(E_z)$ at fixed temperature $T<T_c$ was verified experimentally in Ref. 99 for $T\lesssim 50$ K and for an alternative electric field $E_z\lesssim 0.4$ keV/cm. However, for larger fields, or close to the transition ($T\sim 60$ K) the experimental curves $\Delta M_y(E_z)$ show a nonlinear behavior which cannot be deduced from our model. It may be explained by the fact that, within the experimental conditions (i.e., a relatively strong field at low frequency of 1.5 kHz), the volume percent polarization following the electric field is not negligible and may increase nonlinearly with increasing field and temperature, as the electric coercive field is not an intrinsic property of the crystal. Such an effect can be compared with analogous phenomena evidenced in some ferroelectrics close to the transition point, e.g., to extrinsic peaks of the dielectric constant which are observed at low frequencies (see, for instance, Schmid and Peterman[100]). Let us note that close to the Curie point, Baturov *et al.*[98] find negative values for $\Delta M_y(E_z)$—and thus for α_{yz}—in conformity with the precedingly mentioned variation of $\Delta P_z(E_y)$.

The electric field dependence of the magnetization components is given in Table V(d). One can see that a linear relationship between the magnetization and electric field components can be verified only for $M_z(E_y)$, $M_y(E_z)$, $M_y(E_x)$, and $M_x(E_y)$. No electric field dependence is found for $M_x(E_x,E_z)$, $M_y(E_y)$, and $M_z(E_x,E_y)$. Accordingly, the only nonvanishing magnetoelectric coefficients are

$$\alpha_{zy}=\frac{\partial M_z}{\partial E_y}=\frac{\partial M_y}{\partial E_z}=\alpha_{yz}=\frac{\alpha_0\chi_0^E}{(\chi_0^M)^{-2}}(\delta_1+\delta_2)\rho_1\rho_2\rho_3 \tag{12}$$

and

$$\alpha_{yx}=\frac{\partial M_y}{\partial E_x}=\frac{\partial M_x}{\partial E_y}=\alpha_{xy}=-\frac{\alpha_0\chi_0^E}{(\chi_0^M)^{-2}}(\delta_1-\delta_2)\rho_2\rho_2\rho_3 . \tag{13}$$

It must be pointed out that the equations listed in Tables V(c) and V(d) refer to cubic coordinates. In orthorhombic axes (i.e., with the x and y axes turned by 45° in their plane), one should also detect nonzero values for the α_{xx} and α_{yy} coefficients, as found in Ref. 13. Besides, the vanishing of α_{zz} which is predicted by our model—although it is not an intrinsic property of the magnetoelectric tensor for the m' symmetry[101]—was verified experimentally by Baturov and Al'shin.[13] By contrast the $\alpha_{xz}=0$ value measured by these authors is not allowed by the monoclinic symmetry and may be explained by the existence of antiparallel domains along the z axis. No precise verification of the $(T_c-T)^{3/2}$ behavior expressed by Eqs. (12) and (13) can be performed by comparison with the experimental curves shown in Ref. 13 for the magnetoelectric coefficients, because of the schematic character of these curves, and especially to the lack of experimental points in the vicinity of T_c.

D. Applicability of the model

In summary, a large number of the distinctive macroscopic features of the transition in Ni-I boracite are explained in the framework of the six-component order-parameter model developed in Sec. II. The essential *improper* character assumed for the magnetization and polarization components is fairly well illustrated by the magnitude and temperature (or field) dependence of the preceding quantities, as well as by the form of the corresponding susceptibilities. Some typical magnetic properties of the material (i.e., the asymmetry of the hysteresis loops and the change in sign of the magnetization under suitably oriented magnetic field) appear to be connected to the peculiar $\nu=3$ faintness index which characterizes the coupling between the magnetization and the order parameter. Similarly, the remarkable magnetoelectric properties of Ni-I can be deduced from both the direct and indirect (i.e., through the order parameter) couplings between the magnetization and polarization components.

However, a number of crucial measurements are still needed in order to check more completely the validity of the model and to clarify some unexplained experimental data: (i) More careful verification of the $\frac{3}{2}$ critical index predicted for the magnetization and the magnetoelectric coefficients in the vicinity of T_c is needed.

(ii) Calorimetric measurements confirming the continuous character of the transition suggested by most of the experimental data, but infirmed by the birefringence and magnetic susceptibility curves are needed. In this respect, a reinvestigation of the preceding quantities in single monodomain crystal is desirable.

(iii) A neutron diffraction experiment verifying the

monoclinic symmetry and fourfold increase of the magnetic and chemical cell below T_c, as well as the type of antiferromagnetic ordering predicted in our model is needed (see Sec. VI A).

IV. TRIGONAL BORACITES

In contrast to the case of Ni-I boracite, the transitions evidenced at low temperatures in Co-Cl and Fe-X (X=Cl, Br, I) boracites are assumed to be purely magnetic ones (see Sec. II). As shown in Table II, it is a two-dimensional Brillouin-zone center IC (denoted τ_3) of the paramagnetic group $R3c1'$, which induces the monoclinic low-temperature phase of magnetic symmetry m, the ferroelectric $R3c$ structure remaining essentially trigonal below T_c.[9,56] Accordingly, the corresponding Landau expansion (denoted b in Table III) is expressed as a function of a two-component order parameter (η_1,η_2) which identifies with an antiferromagnetic sublattice ordering. The linear relationship between these components and the mean spin distribution will be discussed in Sec. VI B in connection with the magnetic structure assumed for the monoclinic phase.

As in Dzialoshinskii's theory,[46] the weak ferromagnetic character of the magnetic phases can be described phenomenologically by a bilinear coupling of the magnetization components (M_x,M_y) to the order parameter. Such a coupling, which is written $\delta(\eta_1 M_y-\eta_2 M_x)$ expresses the fact that (η_1,η_2) and $(M_y,-M_x)$ both transform as the same IC τ_3. The set of lower-degree coupling terms between the M_u ($u=x,y,z$) and the η_i are given in Table VI(a). They will allow us to describe the magnetic anomalies observed in the group of boracites under consideration.

The fact that no structural transition (and therefore no spontaneous components of the polarization and strain) takes place at T_c, does not exclude that anomalous temperature dependences may possibly be observed for some dielectric and elastic properties of the materials.[60] Such anomalies, which reflect the influence of the magnetic transition on the structure, are governed by couplings between the order-parameter or the magnetization components on one hand, and the nonspontaneous components of polarization and strain, on the other hand (i.e., the components which already exist in the high-temperature phase). These couplings are listed in Table VI.

A. Magnetic properties

Let us first discuss, in the framework of our model, the magnetic properties of Co-Cl and Fe-X boracites. Such properties were evidenced experimentally by susceptibility,[3,31] hysteresis loop[8] and Faraday rotation[59] measurements. Minimization of $F_1+F_M(\mathbf{H}=\mathbf{0})$ with respect to M_x and M_z yield

$$M_x=\delta\chi_0^M\eta_2$$

and (14)

$$M_y=-\delta\chi_0^M\eta_1\ .$$

In Table III one can see that the equilibrium values, for η_1 and η_2 in the monoclinic phase, are $\eta_1\neq 0$ and $\eta_2=0$. Accordingly the spontaneous magnetization below T_c lies along the y axis, i.e., perpendicular to the polarization P_z which is parallel to the C_3^z axis of the trigonal cell. The respective orientations of P_z and M_y were verified experimentally in Co-Cl boracite through the observation of the ferroelectric-ferromagnetic domain structure.[56] In the same material a recently performed Faraday rotation measurement[59] reveals a $(T_c-T)^{1/2}$ asymptotic variation law for the magnetization, in agreement with Eq. (14), although one can verify a slight discontinuity of the angle of rotation at the 11.5-K transition. The first-order character of the magnetic transition is confirmed for Co-Cl

TABLE VI. Coupling terms for the $R3c1'\rightarrow Cc$ transition in trigonal boracites. The terms are labeled as in Table IV.

$$F_M=\delta(\eta_1M_y-\eta_2M_x)+(\eta_1^2+\eta_2^2)\left[\frac{\mu_1}{2}(M_x^2+M_y^2)+\frac{\mu_2}{2}M_xM_y+\frac{\mu_3}{2}M_z^2\right]+\frac{1}{2\chi_0^M}(M_x^2+M_y^2+M_z^2)-\mathbf{H}\cdot\mathbf{M}$$

$$F_E=(\eta_1^2+\eta_2^2)\left[\delta_1P_z+\frac{\mu_1}{2}(P_x^2+P_y^2)+\frac{\mu_2}{2}P_z^2\right]+\frac{1}{2\chi_0^E}(P_x^2+P_y^2+P_z^2)-P_0P_z-\mathbf{E}\cdot\mathbf{P}$$

$$F_s=(\eta_1^2+\eta_2^2)[\delta_1(e_1+e_2)+\delta_2e_3]+(\text{trigonal elastic energy})-e_1^0e_1-e_2^0e_2-e_3^0e_3-\sigma e$$

$$F_{\mathrm{ME}}=(M_x^2+M_y^2)\left[\alpha_{01}P_z+\frac{\alpha_{04}}{2}(P_x^2+P_y^2)\right]+\alpha_{02}P_zM_z^2+M_xM_y[\alpha_{03}P_z+\alpha_{05}(P_x^2+P_y^2)]$$

$$F_{\mathrm{MS}}=(M_x^2+M_y^2)[\alpha_1e_3+\alpha_4(e_1+e_2)]+\alpha_2e_3M_z^2+M_xM_y[\alpha_3e_3+\alpha_5(e_1+e_2)]$$

$$F_{\mathrm{ES}}=P_z[\lambda_1e_3+\lambda_2(e_1+e_2)]+(P_x^2+P_y^2)[\lambda_3e_3+\lambda_4(e_1+e_2)]$$

$$F_{\eta\mathrm{ME}}=(\eta_1M_y-\eta_2M_x)[\gamma_1P_z+\gamma_2(P_x^2+P_y^2)]$$

and Fe-Cl, by the temperature dependence of the magnetic susceptibility measured by Baturov *et al.*[31] (see below) as well as by the unusually large values obtained by Quezel and Schmid[8] for the ferromagnetic moments at 4.2 K. In this respect, we show in Sec. III that while the ratio $|M_y/\eta_1|$ is expected from the theory[46] to be in the range 10^{-2}–10^{-5}, it is actually about 10^{-1}–10^{-2} for Co-Cl and iron boracites, i.e., of the order of magnitude of the larger values experimentally observed for weak ferromagnets [e.g., in C_2F_3 (Ref. 102)].

The magnetic susceptibility χ^M_{yy} is obtained by minimization of $F_1+F_M(\mathbf{H}\neq\mathbf{0})$ with respect to η_1 and M_y. It yields

$$\chi^M_{yy}\simeq\frac{\chi^M_0}{1-\delta^2\chi^M_0/(\alpha+3\beta\eta_1^2)+\mu_1\chi^M_0\eta_1^2}\ , \tag{15}$$

so that $\chi^M_{yy}\simeq\chi^M_0\alpha/(\alpha-\delta^2\chi^M_0)$ in the paramagnetic phase ($\eta_1=0$). Assuming the transition to be of first order (i.e., $\beta<0$, $\gamma_1+\gamma_2>0$ for the b expansion written in Table III) one obtains for sufficiently negative values of μ_1, the behavior represented by the solid line in Fig. 8. Accordingly, at the transition temperature $T_1=T_c+[3\beta^2/16a(\gamma_1+\gamma_2)]$, the susceptibility undergoes an upward jump on cooling, then increases again as the temperature is lowered. The experimental curves obtained by Baturov *et al.*[31] for the inverse susceptibility in Co-Cl and Fe-Cl boracites clearly illustrate the temperature dependence shown on Fig. 8 for $\chi^M_0(T)$. It should be noted that a second-order transition in these materials would correspond to a *drop* of $\chi^M(T)$ at T_c, and a *decreasing* of the susceptibility when the temperature is lowered (dotted line in Fig. 8).

Under application of a magnetic field parallel to the y axis the corresponding Eq. (14) for M_y must be written as

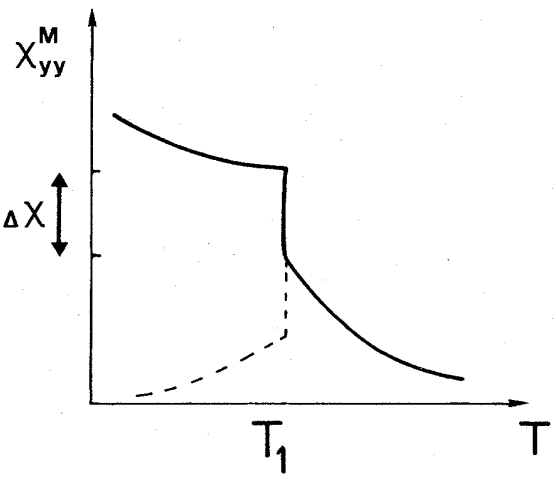

FIG. 8. Temperature dependence of the magnetic susceptibility predicted in trigonal boracites, assuming the transition is first order (solid line) or second order (dotted curve).

$$M_y=\chi^M_0H_y-\delta\chi^M_0\eta_1\ .$$

Accordingly, below T_c the magnetic hysteresis should display symmetric values for the spontaneous magnetization M_s at zero field (i.e., $M_s=\pm\chi^M_0|\eta_1|$). This is verified by the experimental curves found by Quezel and Schmid[8] for the Fe boracites. Large differences in magnitude are observed for the coercive field H_c (4.2 K) for Fe-I (9500 Oe), Fe-Br (1500 Oe), and Fe-I (170 Oe), thus revealing a strong dissimilarity in the magnetocrystalline anisotropy of these compounds.

B. Magnetoelectric properties

Weak dielectric or elastic anomalies are reported for the class of trigonal boracites, in the region of the magnetic transition. From the form of the coupling terms labeled F_E and F_s in Table VI, one can foresee that only secondary structural anomalies should be observed. For, say P_z, one can write below T_c

$$P_z=P_0-\chi^E_0(\delta_1\eta_1^2+\gamma_1\delta\eta_1M_y)\ . \tag{16}$$

The two terms on the right side of Eq. (16) represent, respectively, the polarization already existing above T_c and the order parameter and magnetization-induced polarization. This latter contribution should only modify the slope of the total polarization as a function of the temperature, below T_c. Such weak anomalies are indicative of the purely magnetic character of the transition, assumed in our model, whereas a magnetostructural transition[60] would be accompanied by qualitatively different situations (e.g., the onset of new components of the polarization perpendicular to the C_3^z axis) which have not been observed up to now.

Taking into account the terms F_M, F_E, F_{ME}, and $F_{\eta\mathrm{ME}}$ in Table VI, yields the magnetoelectric relationships:

$$\begin{aligned}&(\Delta P_z)_{E=0}=-\chi^E_0\chi^M_0\gamma_1\eta_1H_y=\chi^E_0\chi^M_0\alpha_{03}\gamma\eta_1H_x\ ,\\&(\Delta M_y)_{H=0}=-\chi^E_0\chi^M_0\gamma_1\eta_1E_z\ ,\\&\text{and}\\&(\Delta M_x)_{H=0}=\chi^E_0\chi^M_0\alpha_{03}\delta\eta_1E_z\ .\end{aligned}\tag{17}$$

Thus, conformably to the symmetry of the magnetoelectric tensor for the monoclinic symmetry m,[101] one obtains the sole nonvanishing magnetoelectric coefficients,

$$\alpha_{zy}=\left[\frac{\partial\Delta P_z}{\partial H_y}\right]_{E=0}=\left[\frac{\partial\Delta M_y}{\partial E_z}\right]_{H=0}=\alpha_{yz}=-\chi^E_0\chi^M_0\gamma_1\delta\eta_1,\tag{18}$$

$$\alpha_{zx}=\left[\frac{\partial\Delta P_z}{\partial H_x}\right]_{E=0}=\left[\frac{\partial\Delta M_x}{\partial E_z}\right]_{H=0}=\alpha_{xz}=\chi^E_0\chi^M_0\alpha_{03}\delta\eta_1\ .$$

The variation of induced polarization ΔP_z at fixed temperature $T=11$ K under application of a magnetic field H_x was measured by Schmid[56] for Co-Cl boracite. It confirms the linear relationship $\Delta P_z(H_x)$ given by Eq. (17). The proportionality of α_{zx} to the order parameter η_1 [Eq. (18)] is also well illustrated by the temperature dependence of α_{zx} given in Ref. 56, provided the "tail" observed above

T_c is attributed to a diffuse behavior possibly connected with defects.[103] Similarly, the humps and negative signs obtained by Baturov *et al.*[31] for the magnetoelectric coefficients (α_{yz} or α_{xz}) on ferroelectric polydomain samples of Co-Cl, Fe-Br, and Fe-Cl boracites, should not be intrinsic properties of the corresponding single domains. These features may be explained by orientational effects of the magnetic domains, or by demagnetization processes.

Thus, the two-component order-parameter model, assuming a purely magnetic pseudoproper transition of the first order in trigonal boracites, is verified in its more essential features by the magnetic and magnetoelectric data available for Co-Cl boracite. More experimental information is needed for the group of iron boracites, and especially for Fe-I, in order to check our theoretical predictions. An essential test would be given by a neutron diffraction experiment verifying the monoclinic magnetic symmetry and the corresponding two-dimensional antiferromagnetic canted ordering (see Sec. VI B).

V. ORTHORHOMBIC BORACITES

Assuming that the paramagnetic phase in this third class of boracites is the orthorhombic phase $Pca2_11'$ (see Sec. II A), one can easily relate the variety of magnetic phases evidenced at low temperatures, to the degrees of freedom of the orthorhombic group at the center of the Brillouin zone. From Tables I and II it can be foreseen that the ferromagnetic symmetry group $m'm2'$ (or $mm'2'$), observed in Ni-Cl,[32] Ni-Br,[20–30] and Co-Br,[29] with the magnetization along the y (or x) axis (i.e., perpendicular to the polarization which lies along the z axis), is induced by the IC τ_4 (or τ_3) of $Pca2_11'$ at the Γ point. On the other hand, the ferromagnetic phase of symmetry $m'm'2$ observed below 8.4 K in Cu-Cl,[35,58] and the antiferromagnetic intermediate phase of symmetry $mm2$ evidenced in Ni-Cl[30,32,57] are respectively related to the IC's τ_2 and τ_1. There remains some uncertainty pertaining to the symmetry of the phase ordered between 16.8 and 30 K in Ni-Br.[20,30] The symmetries of the ferromagnetic phases which were shown to exist in Co-I (Refs. 33 and 44) and Cu-Br,[17] are entirely unknown so far.

As is the case of trigonal boracites, the weak ferromagnetic character of the $m'm'2$ and $m'm2'$ phases[3,8] results from a bilinear coupling between the magnetization components M_x, M_y, and M_z to the order parameter η which corresponds to an antiferromagnetic ordering. In Sec. VI B it is shown that η can be written as linear combinations of the antiferromagnetic couples of components (L_{2z},L_{3y}), (L_{1z},L_{3x}), and (L_{1y},L_{2x}), which transform, respectively, as, M_x,M_y, and M_z. However, η is not a magnetization component, although it has the same symmetry. By contrast, for the $mm2$ phase found in Ni-Cl, the corresponding antiferromagnetic ordering, which is identified with the order parameter η, *is* the symmetry breaking quantity. Besides, as the transitions are assumed to be purely magnetic ones,[60] there will only be *nonlinear* couplings between the order parameter and the nonspontaneous components of polarization and strain: The two latter quantities transform as the identity irreducible rep-

TABLE VII. Coupling terms for the $Pca2_11'\rightarrow(Pca2_1,Pca'2_1',Pc'a'2_1,Pc'a2_1')$ transitions in orthorhombic boracites. Same notation as in Table IV.

$$F_M=\begin{Bmatrix}\tau_1:\\ \tau_2:\ \delta\eta M_z\\ \tau_3:\ \delta\eta M_x\\ \tau_4:\ \delta\eta M_y\end{Bmatrix}+\frac{1}{2\chi_0^M}(M_x^2+M_y^2+M_z^2)-\mathbf{H}\cdot\mathbf{M}$$

$$F_E(\tau_1\rightarrow\tau_4)=\delta\eta^2P_z+\frac{1}{2\chi_0^E}(P_x^2+P_y^2+P_z^2)-\mathbf{E}\cdot\mathbf{P}-P_0P_z$$

$$F_S(\tau_1\rightarrow\tau_4)=\eta^2(\lambda_1e_1+\lambda_2e_2+\lambda_3e_3)+(\text{orthorhombic elastic energy})-\sigma e-(e_1^0e_1+e_2^0e_2+e_3^0e_3)$$

$$F_{\mathrm{ME}}=\begin{Bmatrix}\tau_1:\\ \tau_2:\ \alpha_{01}M_z^2P_z\\ \tau_3:\ \alpha_{01}M_x^2P_z\\ \tau_4:\ \alpha_{01}M_y^2P_z\end{Bmatrix},\quad F_{\mathrm{ES}}=\begin{Bmatrix}\tau_1:\ P_z(\lambda_1e_1+\lambda_2e_2+\lambda_3e_3\\ \tau_2:\\ \tau_3:\ \lambda P_ye_4\\ \tau_4:\ \lambda P_xe_5\end{Bmatrix}$$

$$F_{\mathrm{MS}}(\tau_1\rightarrow\tau_4)=M_u^2(\alpha_1e_1+\alpha_2e_2+\alpha_3e_3)\quad(u=x,y,z)$$

$$F_{\eta\mathrm{ME}}=\begin{Bmatrix}\tau_1:\\ \tau_2:\ \gamma_1\eta M_zP_z\\ \tau_3:\ \gamma_1\eta M_xP_z+\gamma_2\eta P_xM_y\\ \tau_4:\ \gamma_1\eta M_yP_z+\gamma_2\eta M_zP_y\end{Bmatrix}$$

resentation of the crystallographic group $Pca2_1$.

Using the single components order parameter $F_1(\eta)$ (labeled a in Table III), and the coupling terms worked out in Table VII, between η and M_u, P_u ($u=x,y,z$) or e_i ($i=1,6$), enables us to discuss the physical anomalies observed at the transitions. As the phenomenological approach of this class of compounds is very similar to the one performed for trigonal boracites, we shall restrict ourselves to discuss the predictions of the theoretical model, without giving details of the mathematical procedure.

A. Ni-Cl, Ni-Br

Although there are no direct neutron diffraction data on the structures of the two low-temperature magnetic phases of Ni-Cl, there exist sufficient measurements to deduce their characteristics. Thus, the weak ferromagnetic nature of the phase stable below 8—10 K is concluded from: (i) The observation of ferromagnetic domains[30] in the interior of the ferroelectric-ferroelastic domains (Fig. 3) showing a spontaneous magnetization $M_s \| y$ perpendicular to the polarization $P_s \| z$, according to the ferromagnetic group $m'm2'$. (ii) Faraday rotation,[30] magnetization,[57] coercive field,[32] and susceptibility[3,8,57] measurements which reveal typical weak-ferromagnetic behavior with weak magnetization (19 G at 4.5 K) and coercive field (600 Oe at 8.5 K).[8] (iii) A complete set of magnetoelectric data[32] confirms the symmetry $m'm2'$, as only the two-components α_{32} and α_{23} of the magnetoelectric tensor[101] are found to be nonvanishing.

The antiferromagnetic character of the intermediate 10—25 K phase in Ni-Cl, can also be strongly conjectured on the basis of (i) magnetic susceptibility data[3,8,57] which reveal an antiferromagnetic coupling; (ii) the disappearance of the coercive field on increasing temperature at about 10 K; (iii) magnetic torque curves[57] suggesting a collinear antiferromagnetic order, with the sublattice moment directed along the z direction. The preceding results suggest an $mm2$ magnetic point group, which is confirmed by the observed linearity up to 6 kOe of the magnetoelectric effect in the range 9—25 K[32] (i.e., the magnetoelectric tensor has the same nonvanishing components for the $mm2$ and $m'm2'$ symmetries), as well as from the symmetry analysis (see Table II).

For Ni-Br, there are apparently contradictory data concerning the magnetic ordering taking place below 30 K. From the earlier results[20,30] the lower-temperature phase stable below 16.8 K appeared to be isomorphic with the weak ferromagnetic phase of Ni-Cl. In this respect, the disappearance of the coercive field at 16.8 K (Ref. 20) suggested, as for Ni-Cl, an antiferromagnetic intermediate phase between 16.8 and 30 K. This conclusion is however inconsistent with the nonvanishing of Faraday rotation observed in this temperature range[30,99] as well as with the two steps variation appearing in the α_{32} magnetoelectric coefficient as a function of temperature.[20] More recent measurements on a sample cut differently[99] reveal a nonzero coercive field up to 30 K, with also a two stage decreasing on heating, whereas the magnetoelectric coefficient α_{23} seems to increase continuously from 30 to 4 K. The preceding behavior suggests a competition between a number of phases displaying close regions of stability, namely two weak-ferromagnetic phases of symmetry $m'm2'$ and an antiferromagnetic phase of symmetry $mm2$.

The temperature dependence of the antiferromagnetic sublattice magnetization which identifies to η corresponds in our model to a standard $(T_c-T)^{1/2}$ variation law. When the antiferromagnetic phase is the first to take place the subsequent transition toward a weak-ferromagnetic phase (e.g., at $T_c \sim 9$ K in Ni-Cl) may still be associated with the continuous onset of a spontaneous magnetization M_y, as the sublattice magnetization, and hence the order parameter η to which M_y is coupled, is distinct from the one which has taken place in the antiferromagnetic phase (i.e., the antiferromagnetic sublattices in the $mm2$ and $m'm2'$ phases transform as *different* IC's of the $Pca2_11'$ group (τ_1 and τ_4, respectively). Such a feature is apparently verified in Ni-Cl, both by the temperature dependence of M_y deduced from magnetic torque,[57] and by the Faraday rotation curve shown in Ref. 30. Accordingly, standard antiferromagnetic behavior[104] should be expected for the magnetic susceptibility χ^M at the paramagnetic-antiferromagnetic transition, while at T_{c2} one should have a weak-ferromagnetic susceptibility following a law of the type given by Eq. (15). Although the paramagnetic susceptibility measured for Ni-Cl (Ref. 3) indeed shows a Curie-Weiss—type behavior, the absence of susceptibility data across the sequence of magnetic transitions does not allow to verify the preceding theoretical prediction.

The coupling between η and the polarization and strain components [P_z, and e_i ($i=1,3$)] are shown from Table VII to be described by equations of the type (16), where the variations ΔP_z and Δe_i induced by the magnetic transitions, are proportional to the square of the order parameter η. Thus, as for trigonal boracites, one should detect only weak dielectric and elastic anomalies at the magnetic transition temperatures. Actually, one observes a clearcut drop of the birefringence curve, around 9 K in Ni-Cl.[30] In Ni-Br, two distinct kinks are detected around 17 and 28 K, on the slope of the spontaneous polarization.[20] It can be noted that in both cases the magnetostructural anomaly results in a drop on the curve representing the temperature dependence of the nonspontaneous tensors (i.e., polarization or strain), which is indicative of a positive value for the coupling coefficient in Eq. (16).

The magnetoelectric properties evidenced in Ni-Cl and Ni-Br can be expressed in the weak ferromagnetic phase by the equations

$$\Delta P_y = -\chi_0^M \chi_0^E \gamma_2 \eta H_z \tag{19}$$

and

$$\Delta P_z = -\chi_0^M \chi_0^E (\gamma_1 \eta + \alpha_{01} \chi_0^M) H_y \tag{20}$$

deduced from the F_{ME} and $F_{\eta\mathrm{ME}}$ terms in Table VII. The preceding equations yield as nonvanishing linear magnetoelectric coefficients

$$\alpha_{23}=\left[\frac{\partial P_y}{\partial H_z}\right]_{E=0}=-\chi_0^M\chi_0^E\gamma_2\eta \tag{21}$$

and

$$\alpha_{32}=\left[\frac{\partial P_z}{\partial H_y}\right]_{E=0}=-\chi_0^M\chi_0^E\gamma_1\eta\ . \tag{22}$$

The linearity of the magnetoelectric effect expressed by Eq. (19) has been verified[32] at any $T<T_c$. Furthermore, the temperature dependence of α_{23} measured in Ref. 32 follows closely the $(T_c-T)^{1/2}$ law given by Eq. (21). The continuous vanishing of α_{23} at 9 K, and its zero value in the antiferromagnetic phase, confirms our assumption that the two magnetic phases are associated with *distinct* antiferromagnetic orderings. Actually, as can be seen in Table VII, there is *no* linear magnetoelectric coupling F_{ME} and $F_{\eta\mathrm{ME}}$, corresponding to the IC τ_1, which is related to the $mm2$ phase.

Equation (20) predicts that the polarization ΔP_z should vary nonlinearly under strong magnetic field applied in the y direction. The experimental curves $\Delta P_z(H_y)$ measured at 4.5 and 8.4 K (i.e., in the $m'm2'$ phase) as well as at 16.5 K (in the $mm2$ phase), show, on the contrary, a linear variation up to $H_y=6$ kOe.[32] This would suggest that the α_{01} coefficient is small with respect to γ_1, or in other words, that the "direct" magnetoelectric effect $(P_zM_y^2)$ is small in comparison to the "indirect" one (ηM_yP_z). Besides, the change of sign of the slope $\Delta P_z/H_y$ from 8.4 to 16.5 K, is consistent with the assumption of a distinct sublattice ordering in the two phases. On the other hand, the temperature dependence of α_{32} shown in Ref. 32 differs strongly from the theoretical law given by Eq. (22). It reveals a peak around 9 K and small negative values for ΔP_z between 10 and 25 K.[32] Such a behavior may be indicative of the fact that a magnetic field applied along the y axis induces a magnetoelectric contribution of the antiferromagnetic sublattice existing in the $mm2$ phase, whereas this contribution is absent when the field is applied along the z direction. Hence, the apparently contradictory shapes of $\alpha_{23}(T)$ and $\alpha_{32}(T)$ may be reconciled by assuming that the sublattice magnetization in the antiferromagnetic phase, lies along the z direction, as was proposed by Haida *et al.*,[57] so that it would be mainly affected by magnetic field applied in the perpendicular direction.

The preceding assumption, which is discussed in Sec. III, would also allow to interpret the magnetoelectric measurement obtained for Ni-Br.[20,99] In this material, application of a magnetic field along the y direction induces a magnetoelectric contribution of the antiferromagnetic sublattice in the range 16.8—30 K, which appears in the α_{32} coefficient.[20] By contrast a magnetic field applied along z would favor the stability below 30 K, of the noncompensated antiferromagnetic sublattice which give rise to the weak-ferromagnetic component M_y. Accordingly, the magnetoelectric coefficient α_{23} should follow a continuous variation given by Eq. (20), as is observed experimentally.[99]

B. Co-Br, Cu-Cl

A single magnetic phase is reported for each of these two compounds.[29,35] In Co-Br boracite, the ferromagnetic-ferroelectric domain pattern[29] shows a magnetization perpendicular to the polarization; the phase thus is of symmetry $m'm2'$ or $mm'2'$. The weak ferromagnetic character of the $T_c=16$ K transition is confirmed by magnetic moment,[8] coercive field[8] and Faraday rotation[29] measurements. The latter reveals a continuous increase of the rotation angle from T_c. Such a smooth onset of the magnetization may explain the failure to observe any anomaly in the birefringence curve.[29]

The magnetic phase evidenced below about 8 K in Cu-Cl, is interpreted by Haida *et al.*[35] as corresponding to the symmetry $m'm'2$, which is induced by the τ_2 IC of the $Pca2_11'$ group. Following these authors the magnetic moment should be aligned along the z direction, i.e., parallel to the polarization. This result is deduced from magnetic torque curves.[35] Unpublished data from Haida and Kohn[58] also reveal a magnetization curve with a typical second-order $(T_c-T)^{1/2}$ variation. More recent unpublished magnetoelectric measurements by Rivera and Schmid[58] confirm the existence of a spontaneous magnetization component along the z axis. More experimental data are needed for further interpretation.

C. Co-I, Cu-Br

The weak ferromagnetic character of the phases evidenced below 38 and 24 K, respectively, in Co-I and Cu-Br boracites, is attested to by magnetic moment and coercive field measurements.[8] However, the data are still overly incomplete for definite conclusions to be drawn on the symmetry of these phases. The dielectric measurements reporting marked anomalies of the permittivity and polarization around 24 K suggest thereby a strong magnetoelectric effect for the corresponding magnetic transition in Cu-Br. In Co-I, a spontaneous magnetization curve[33] shows two distinct phases in the range 38—29 K, and below 29 K. Magnetoelectric anomalies,[44] dielectric permittivity curves,[17,33] and neutron diffraction data[84] confirm a two-step phase sequence. However, the preceding results have been obtained from polydomain samples, so that the detection of magnetization components along z and x (or y), as well as the nonzero values found for most of the magnetoelectric tensor components (in agreement with a *triclinic* symmetry) require confirmation by single domain crystals.

In this third group of boracites the variety of theoretical situations predicted in our model, related to the fact that four possible irreducible degrees of freedom may be involved, is illustrated by an apparent complexity of the experimental data. In two members of the group, namely Ni-Cl and Co-Br, for which the experimental situation is presently the more firmly established, the magnetic and magnetoelectric measurements confirm fairly well the theoretical model of a single-component order parameter, coupling linearly to the magnetization and to the nonspontaneous polarization. In the other compounds the discrepancy between some magnetic and magnetoelectric data of different origins, can be understood by the fact

that magnetic phases connected to different degrees of freedom are observed. These phases which seem to have close regions of stability, appear to be very sensitive to the experimental conditions and, in particular, to the orientation of the applied magnetic field and to the existence of domains. In these materials, magnetic and magnetoelectric experiments have thus to be performed with a particular care as regarding the preceding "perturbations." A better knowledge of the antiferromagnetic sublattices involved in each orthorhombic magnetic phase, which is discussed in Sec. VI C, should also help to work in "unperturbed" conditions.

VI. MICROSCOPIC NATURE OF THE ORDER PARAMETER IN MAGNETIC BORACITES: LATENT ANTIFERROMAGNETISM AND WEAK FERROMAGNETISM

The Landau theory of boracites developed in the previous sections differs in many respects from the usual phenomenological approaches to magnetic phase transitions. For example, in the works of Dzialoshinskii,[46,47,105] the Landau expansion F is constructed from invariant combinations of the magnetic moments, the distribution of which is known *a priori*. In the Kovalev method,[106] although F is composed of invariants of the functions making up the irreducible representations of the crystallographic group under consideration, one has to know the location and orientation of the magnetic moments. In both cases, the knowledge of the detailed magnetic structure is a necessary preliminary in order to deduce the nature (exchange or relativistic) of the forces which are mainly responsible for the magnetic ordering. On the other hand, statistical mechanics models[107] start from assumptions on the form of the fundamental interactions between the neighboring moments, which lead in turn to predictions of the macroscopic features of the system.

Our approach, in contrast, is adapted to the description of magnetic transitions in systems where a number of macroscopic properties are known (e.g., the symmetries of the phases, the temperature dependence and magnitude of the spontaneous tensors), but where the average spin distribution is still unknown. Starting from the observed modifications, a group theoretical and thermodynamic analysis enables us to determine the symmetry of the irreducible degree of freedom governing the transition. Then, on the basis of the available experimental data, we postulate the physical mechanism representing the order parameter and deduce its coupling with the other (secondary) degrees of freedom involved in the transition. As shown in Secs. III, IV, and V, it allows us to account for most of the macroscopic anomalies characterizing the transition, and accordingly to verify our initial assumption on the nature of the order parameter.

In this section we show that it is possible to specify, to a certain extent, the magnetic ordering which takes place at low temperature in boracites, starting only from the crystallographic structure of the paramagnetic phase, and thus to deduce the type of interactions responsible for the transition. In this respect, it appears from the previous sections that, on a phenomenological basis, two main situations have been found among magnetic boracites. On one hand, the transition in Ni-I boracite was described as an *improper* magnetostructural transition associated to a Brillouin-zone boundary IC. On the other hand, the two remaining classes of transitions were treated as *pseudoproper* magnetic transitions, induced by zone-center instabilities. We now examine the basic physical implications of such a distinction.

A. Latent antiferromagnetism in Ni-I boracite

In the paramagnetic phase, the cubic primitive cell of Ni-I boracite is a rhombohedron of volume V (Fig. 4) containing two formula units. Thus the conventional cell[71] $F\bar{4}3c1'$ contains eight formula units with 24 magnetic ions Ni^{2+}. At $T_c = 61.5$ K the structure becomes monoclinic (Cc'), the primitive monoclinic cell having the same volume as the conventional cubic cell. We can assume, without loss of generality, that the lowering of symmetry taking place at T_c is entirely connected with the displacement of the nickel ions. The 24 metallic ions will thus be distributed among 12 independent monoclinic sublattices. The positions of the ions forming each sublattice are given in Table VIII. In Figs. 9(a) and 9(b), the magnetic ions are represented in projection on the pseudocubic plane (001), and within the monoclinic cell, respectively. Having regard to their structural environment, the 12 independent nickel ions form three groups, denoted (1,2,3,4), (5,6,7,8), and (9,10,11,12) in Fig. 9, located inside mixed oxygen halogen octahedra, the axes of which are parallel or at 45° to the monoclinic plane. The three groups of atoms lie, respectively, in planes perpendicular to the cubic z direction, and to the x direction ($x=0$ and $x=\frac{1}{2}$).

The magnetic structure of the crystal in the low-temperature phase is completely determined if the spins of

TABLE VIII. Coordinates of the nickel ions associated with the 24 average spins s_i ($i=1$—24) in the monoclinic Cc (C_s^4) cell of Ni-I boracite. The coordinates are given with respect to the cubic axes x,y,z.

s_1: $\frac{1}{4},\frac{1}{4},0$	s_{13}: $\frac{1}{4},\frac{1}{4},\frac{1}{2}$
s_2: $\frac{3}{4},\frac{3}{4},0$	s_{14}: $\frac{3}{4},\frac{3}{4},\frac{1}{2}$
s_3: $\frac{1}{4},\frac{3}{4},0$	s_{15}: $\frac{3}{4},\frac{1}{4},\frac{1}{2}$
s_4: $\frac{3}{4},\frac{1}{4},0$	s_{16}: $\frac{1}{4},\frac{3}{4},\frac{1}{2}$
s_5: $0,\frac{1}{4},\frac{1}{4}$	s_{17}: $\frac{1}{4},0,\frac{3}{4}$
s_6: $0,\frac{1}{4},\frac{3}{4}$	s_{18}: $\frac{1}{4},0,\frac{1}{4}$
s_7: $0,\frac{3}{4},\frac{1}{4}$	s_{19}: $\frac{3}{4},0,\frac{3}{4}$
s_8: $0,\frac{3}{4},\frac{3}{4}$	s_{20}: $\frac{3}{4},0,\frac{1}{4}$
s_9: $\frac{1}{2},\frac{1}{4},\frac{1}{4}$	s_{21}: $\frac{1}{4},\frac{1}{2},\frac{3}{4}$
s_{10}: $\frac{1}{2},\frac{1}{4},\frac{3}{4}$	s_{22}: $\frac{1}{4},\frac{1}{2},\frac{1}{4}$
s_{11}: $\frac{1}{2},\frac{3}{4},\frac{1}{4}$	s_{23}: $\frac{3}{4},\frac{1}{2},\frac{3}{4}$
s_{12}: $\frac{1}{2},\frac{3}{4},\frac{3}{4}$	s_{24}: $\frac{3}{4},\frac{1}{2},\frac{1}{4}$

the ions belonging to each sublattice are given. Following the method used by Dzialoshinskii in a number of papers[46,47,105] we shall symbolize the spins by $s_1,s_2,\ldots,s_{12}$ and denote by $s_{13},s_{14},\ldots,s_{24}$ the spins of the ions, respectively, obtained by reflection in the monoclinic plane $\sigma_{\bar{x}z}$. Assuming that the s_i are small close to T_c, the Landau free energy F can be expanded as power series of the s_i components s_{iu} $(u=x,y,z)$. Let us introduce the auxiliary vectors M^α and L_j^α $(j,\alpha=1,2,3)$ defined by the equations

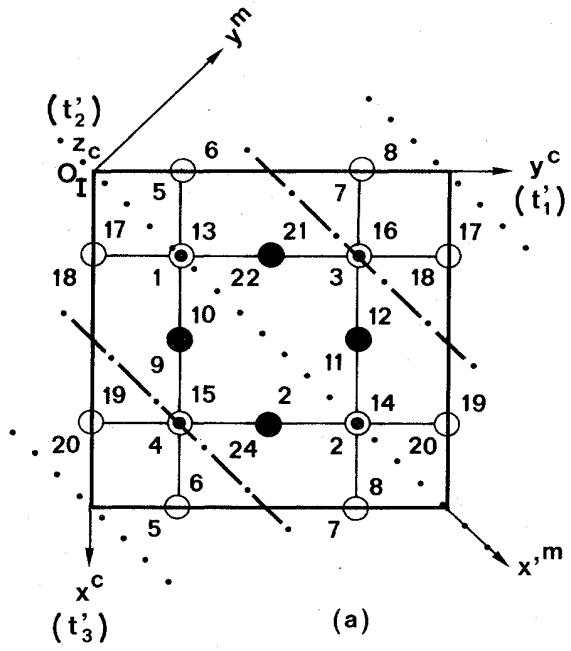

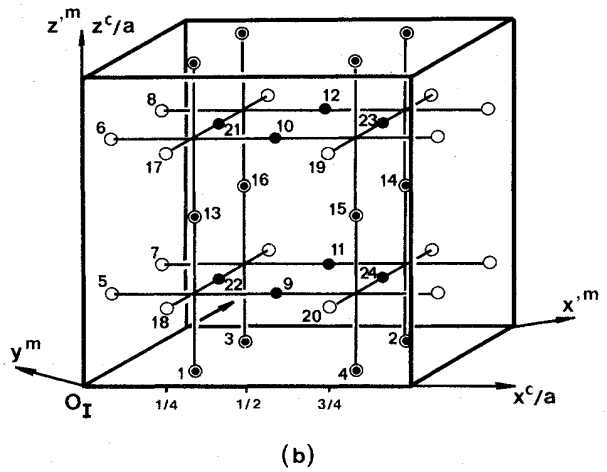

FIG. 9. Position of the 24 nickel ions in the monoclinic Cc (C_s^4) phase of Ni-I boracite, neglecting the monoclinic deformation with respect to the cubic phase. (a) Projection on the xy cubic plane. Numbers below or above the metals indicate whether they are located (i) at $z=\frac{1}{4}$ or $z=\frac{3}{4}$ for metals 5—12 and 17—24, and (ii) at $z=0$ or $z=\frac{1}{2}$ for metals 1—4 and 13—16. (b) Positions of the metals within the volume of the monoclinic cell. In the two figures the cubic (x^c,y^c,z^c) and monoclinic (x'^m,y'^m,z'^m) axes have the same origin (O_I) as in Ref. 5.

$$
\begin{aligned}
&L_1^1=s_1+s_{13}+s_2+s_{14}-s_3-s_{15}-s_4-s_{16}\ ,\\
&L_2^1=s_1+s_{13}-s_2-s_{14}+s_3+s_{15}-s_4-s_{16}\ ,\\
&L_3^1=s_1+s_{13}-s_2-s_{14}-s_3-s_{15}+s_4+s_{16}\ ,\\
&L_j^2=L_j^1(s_{i+4}),\quad L_j^3=L_j^1(s_{i+8})\\
&\qquad\qquad (j=1,2,3)\ \ (i=1\text{—}4 \text{ and } 12\text{—}16)\ ,\\
&M^1=s_1+s_{13}+s_2+s_{14}+s_3+s_{15}+s_4+s_{16}\ ,\\
&M^2=M^1(s_{i+4}),\quad M^3=M^1(s_{i+8})\ \ (i=1\text{—}4 \text{ and } 12\text{—}16)\ .
\end{aligned}
\tag{23}
$$

It is obvious that the vector $M=M^1+M^2+M^3$ represents the total magnetization moment of the monoclinic unit cell below T_c. It transforms as the three-dimensional vector corepresentation of the $F\bar{4}3c1'$ group, at the Brillouin-zone center, labelled τ_5 in Table II. On the other hand, it can easily be found that the *reducible* corepresentation given by the antiferromagnetic vectors L_j^α decomposes into *two* IC's of the $F\bar{4}3c1'$ group at the X (k_{10}) point of the face-centered Brillouin zone. More precisely, $(L_{1x}^\alpha,L_{2y}^\alpha,L_{3z}^\alpha)$ transform as the three-dimensional IC denoted τ_3 in Table II, whereas the six-dimensional IC τ_1 describes the transformation properties of the components $(L_{1y}^\alpha,L_{1z}^\alpha,L_{2x}^\alpha,L_{2z}^\alpha,L_{3x}^\alpha,L_{3y}^\alpha)$. As already noted in Ref. 108, each of the sets of L_j^α projections are distributed over the three arms of the star[69] $\mathbf{k}_{10}^*$, namely $\mathbf{k}_{10}^1=(0,0,\pi/a)$, $\mathbf{k}_{10}^2=(0,\pi/a,0)$, $\mathbf{k}_{10}^3=(\pi/a,0,0)$ in the Kovalev notation.[109]

As τ_1 was found to induce the phase transition in Ni-I boracite (Sec. II B), we can thus work out the linear relationships between the L_j^α projections and the abstract order-parameter components η_i $(i=1,6)$ used in Secs. II and III. Identifying the basis of the six-dimensional IC τ_1 spanned, respectively, by the η_i and the L_{ju}^α $(u=x,y,z)$ yields

$$
\begin{aligned}
&\eta_1=L_{3x}^\alpha+L_{3y}^\alpha,\quad \eta_3=L_{1z}^\alpha-L_{1y}^\alpha,\quad \eta_5=L_{2z}^\alpha-L_{2x}^\alpha\ ,\\
&\eta_2=L_{3x}^\alpha-L_{3y}^\alpha,\quad \eta_4=L_{1y}^\alpha+L_{1z}^\alpha,\quad \eta_6=-L_{2x}^\alpha-L_{2z}^\alpha\ ,
\end{aligned}
\tag{24}
$$

where $\alpha=1,2,3$.

Using (24), we can express the expansion $F(\eta_i,M_x,M_y,M_z)$ (see Tables III and IV) in terms of the $L^\alpha,M^\alpha,M_u^\alpha,L_{ju}^\alpha$, separating its exchange and anisotropic parts. We find $F=\sum_\alpha(F_{\text{ex}}^\alpha+F_{\text{an}}^\alpha)$. For $\alpha=1,2,3$, one has, omitting the superscript α,

$$F_{\rm ex}=\frac{a}{2}\sum_j (L_j)^2+\frac{B_1}{4}\left[\sum_j (L_j)^2\right]^2+\frac{B_2}{4}\sum_j (L_j)^4+\frac{B_3}{4}\sum_{i\neq j}(L_iL_j)^2+\frac{C}{2}M^2$$
$$+D[(ML_1)L_2L_3+(ML_2)L_1L_3+(ML_3)L_1L_2]+\frac{E_1}{2}(M)^2\left[\sum_j (L_j)^2\right]+\frac{E_2}{2}\sum_j (ML_j)^2\,, \tag{25}$$

where the B_i, C, D, E_i are constant coefficients and $a\sim(T-T_c)$. We write

$$F_{\rm an}=\tfrac{1}{2}\alpha(L_{1y}^2+L_{1z}^2+L_{2x}^2+L_{2z}^2+L_{3x}^2+L_{3y}^2)+\tfrac{1}{4}\beta_1(L_{1y}^4+L_{1z}^4+L_{2x}^4+L_{2z}^4+L_{3x}^4+L_{3y}^4)$$
$$+\tfrac{1}{2}\beta_2(L_{1y}^2L_{1z}^2+L_{2x}^2L_{2z}^2+L_{3x}^2L_{3y}^2)+\tfrac{1}{2}\beta_3[(L_{1y}^2+L_{1z}^2)(L_{2x}^2+L_{2z}^2+L_{3x}^2+L_{3y}^2)+(L_{2x}^2+L_{2z}^2)(L_{3x}^2+L_{3y}^2)]$$
$$+\tfrac{1}{2}\beta_4[(L_{3x}^2-L_{3y}^2)(L_{1z}^2-L_{1y}^2+L_{2z}^2-L_{2x}^2)+(L_{1z}^2-L_{1y}^2)(L_{2x}^2-L_{2z}^2)]$$
$$+\tfrac{1}{2}\beta_5[(L_{3x}^2-L_{3y}^2-L_{1z}^2+L_{1y}^2)(L_{1z}^2+L_{1y}^2-L_{2x}^2-L_{2z}^2)+(L_{2z}^2-L_{2x}^2)(L_{3x}^2+L_{3y}^2-L_{1y}^2-L_{1z}^2)]$$
$$+\delta_1[M_x^2(L_{1z}^2L_{2z}^2L_{3x}^2+L_{1y}^2L_{2x}^2L_{3y}^2)+(L_{3x}^2+L_{3y}^2)(L_{1y}^2L_{2x}^2M_y^2-L_{1y}^2L_{2z}^2M_z^2)]$$
$$+\delta_2[M_x^2(L_{1y}^2L_{2x}^2L_{3y}^2-L_{1z}^2L_{2z}^2L_{3x}^2)+M_y^2L_{1y}^2L_{2x}^2(L_{3x}^2+L_{3y}^2)+M_z^2(L_{1y}^2L_{2z}^2L_{3x}^2-L_{1z}^2L_{2x}^2L_{3y}^2)]\,. \tag{26}$$

$F_{\rm ex}$ contains only terms which do not depend on the orientation of the vectors L^α and M^α, i.e., of the orientation of the spins with respect to the crystal axes. They represent exchange interactions. The terms in $F_{\rm an}$ arise from relativistic spin-lattice interaction and magnetic dipole interaction, and determine the magnetic anisotropy of the crystal.[110] As α/a, which approximates the ratio of the magnetic anisotropy energy to the exchange energy, is proportional[111] to v^2/c^2 (i.e., the ratio of the speed of the electrons to the speed of the light), the discussion of F must distinguish two intervals of temperature below T_c:[47] one, close to T_c, in which the relativistic interactions cannot be neglected, and another one, not too close to T_c, where the relativistic terms are negligible. Let us summarize the main results obtained from the minimization of (25) and (26) in connection with the interpretation of the transition in Ni-I boracite.

(i) At $T_c=61.5$ K, where a vanishes, the components of L_i^α become nonzero. The L_i^α vary as $L_i^\alpha\sim(T_c-T)^{1/2}$. Since $F_{\rm ex}^\alpha$ contains an invariant linear in M^α, a nonzero spontaneous magnetic moment will arise simultaneously with the appearance of the L_i^α, that will be of exchange origin. The expression for M^α is

$$M^\alpha=-\frac{D}{C}[L_1^\alpha(L_2^\alpha L_3^\alpha)+L_2^\alpha(L_1^\alpha L_3^\alpha)+L_3^\alpha(L_1^\alpha L_2^\alpha)]\,,$$

which is proportional to $(T_c-T)^{3/2}$. The absolute minimum of $F_{\rm ex}$ associated with this nonzero magnetization corresponds to

$$L_1^\alpha=\pm L_2^\alpha=\pm L_3^\alpha\,. \tag{27}$$

Introducing (27) into (23) leads to

$$s_i+s_{i+12}=\tfrac{1}{4}(M^\alpha\pm 3L_1^\alpha)$$

and (28)

$$s_j+s_{j+12}=\tfrac{1}{4}(M^\alpha\pm L_1^\alpha)\quad (j\neq i)\,,$$

where the number i is determined by the signs in Eq. (27) (e.g., for $L_1^\alpha=L_2^\alpha=L_3^\alpha$, $i=1$, $j=2,3,4$). From Eqs. (28) it can be seen that the average spins of the ions can be divided into two groups, the absolute magnitude of the spins differing from one group to the other. Such a property is usual for ferrimagnets. However, here the spins are associated with one identical type of magnetic ions, which is found in equivalent crystallographic positions in the paramagnetic phase. This is in contrast with the situation found in standard ferrimagnets such as ferrites or garnets (see, for instance, Ref. 107). Dzaloshinskii and Man'ko[47] suggested to denominate this new type of uncompensated antiferromagnetism, *latent antiferromagnetism*. As noted by these authors, no confusion should be made with ferrimagnetism because of the peculiar temperature variation of the magnetization in the vicinity of T_c. However, from the experimental data on Ni-I (Sec. III A), it appears that the interval in which the $(T_c-T)^{3/2}$ law holds, is very narrow, and may escape detection. Another distinctive feature of latent antiferromagnetic materials that was partly overlooked by the authors of Ref. 47, is that, despite its exchange origin the magnetization must be expected to assume very weak values at any temperature below T_c. This is connected with the improper character of the transition, i.e., to the fact that M results from a coupling to the third power of the antiferromagnetic sublattices.

In Ni-I boracite (see Table IX) the magnetization at 4.2 K is found to be about 0.9 G,[79,112] which represents 1% of the nominal value (i.e., the value of the saturation magnetization with all the magnetic moments parallel). In the ferromagnets Fe_3O_4 (Ref. 113) and $Y_3Fe_5O_{12}$,[114] the numerical values found for M are, respectively, about 5×10^3 and 2×10^3 G. No other experimental example of latent antiferromagnetic material, displaying a spontaneous magnetization, is known, that would allow to check if the weak value found for M in Ni-I boracite corresponds to some standard order of magnitude. In UO_2, a potential example of a latent antiferromagnet[47,115,116] no magnetization was found. It is worthwhile mentioning that a nominal value of 10^{-2} corresponds to what is expected in weak ferromagnets.[46] Nevertheless, one should be able to

TABLE IX. Magnetic data for the three subclasses of boracites [column (a)]. Effective magnetic moment: (b) theoretical value $\mu_{\text{eff}}=2\sqrt{s(s+1)}$; (c) μ_{eff} deduced from low-temperature susceptibility measurements (Ref. 8). (d) and (e) Measured magnetization at 4.2 K in emu/g, respectively and G. (f) Ratio of the measured magnetization to the saturation magnetization (Ref. 104).

(a)	(b)	(c)	(d)	(e)	(f)
Ni-I	2.83	4.15	0.016	0.9	1.0×10^{-2}
Fe-Cl	4.9	5.52	5.8	258	4.2×10^{-2}
Fe-Br		5.60	8.5	414	6.7×10^{-2}
Fe-I		5.70	2.6	137	2.3×10^{-2}
Co-Cl	3.87	5.15	8.8	419	8.7×10^{-2}
Co-Br	3.87	5.49	9.5	482	1.0×10^{-1}
Co-I		5.94	1.7	94	2.0×10^{-2}
Ni-Cl	2.83	3.69	0.4	19	6.0×10^{-3}
Ni-Br		3.63	2.15	111	3.4×10^{-3}
Cu-Cl	1.73	2.35	0.015 (0.07)	0.08	5.0×10^{-4}
Cu-Br		2.22	0.08	4.06	3.0×10^{-3}

distinguish latent antiferromagnets from weak ferromagnets by neutron diffraction data, as in the latter class of materials the magnetization results from a canting of antiferromagnetic sublattices having the same magnitude. Moreover, a systematic analysis[68] shows that latent antiferromagnetic transitions should always be accompanied by a structural transition. This transition may lower the point group of the crystal (as in Ni-I boracite), or be associated only to a breaking of the translational symmetry.

(ii) The orientation of the vectors L_i below T_c is determined by the relativistic invariants L_{iu}^{α} in (26). We know from Sec. II (see Table III) that the monoclinic phase in Ni-I boracite corresponds to the equilibrium values $\eta_1\neq0$, $\eta_2=0$, $\eta_3=\eta_4=-\eta_5=\eta_6\neq0$, $\eta_1\neq\eta_i$ $(i=3-6)$.

In terms of the L_{iu}, one attains from (24),

$$L_{1y}^{\alpha}=0,\ L_{2x}^{\alpha}=0,\ L_{3x}^{\alpha}=L_{3y}^{\alpha},\ L_{1z}^{\alpha}=-L_{2z}^{\alpha}\ ,$$
$$L_{3x}^{\alpha}\neq(L_{1x}^{\alpha},L_{2y}^{\alpha},L_{1z}^{\alpha},L_{2z}^{\alpha},L_{3z}^{\alpha})\ . \tag{29}$$

On the other hand, one finds as in Sec. II B,

$$M_x^{\alpha}\neq M_z^{\alpha}\neq0,\quad M_y^{\alpha}=0\ . \tag{30}$$

Substituting (29) and (30) in Eqs. (23) yields the following relationships among the sublattices corresponding to $\alpha=1$:

$$\begin{aligned}
&s_{1x}+s_{13x}=\tfrac{1}{4}\{M_x^1+L_{1x}^1+L_{3x}^1\},\ s_{1y}+s_{13y}=\tfrac{1}{4}\{L_{2y}^1+L_{3x}^1\},\ s_{1z}+s_{13z}=\tfrac{1}{4}\{M_z^1+L_{3z}^1\}\ ,\\
&s_{2x}+s_{14x}=\tfrac{1}{4}\{M_x^1+L_{1x}^1-L_{3x}^1\},\ s_{2y}+s_{14y}=\tfrac{1}{4}\{-L_{2y}^1-L_{3x}^1\},\ s_{2z}+s_{14z}=\tfrac{1}{4}\{M_z^1+2L_{1z}^1-L_{3z}^1\}\ ,\\
&s_{3x}+s_{15x}=\tfrac{1}{4}\{M_x^1-L_{1x}^1-L_{3x}^1\},\ s_{3y}+s_{15y}=\tfrac{1}{4}\{L_{2y}^1-L_{3x}^1\},\ s_{3z}+s_{15z}=\tfrac{1}{4}\{M_z^1-2L_{1z}^1-L_{3z}^1\}\ ,\\
&s_{4x}+s_{16x}=\tfrac{1}{4}\{M_x^1-L_{1x}^1+L_{3x}^1\},\ s_{4y}+s_{16y}=\tfrac{1}{4}\{-L_{2y}^1+L_{3x}^1\},\ s_{4z}+s_{16z}=\tfrac{1}{4}\{M_z^1+L_{3z}^1\}\ ,
\end{aligned} \tag{31}$$

and the same relationships for the average moments s_{i+4} and s_{i+8} $(i=1-4,12-16)$ with $\alpha=2$ and $\alpha=3$, respectively.

Equations (31), and the similar equations for $\alpha=2,3$, provide some information about the magnetic structure of the monoclinic phase in Ni-I boracite. Thus, the noncompensation of the antiferromagnetic sublattices appear on the x and z projections, whereas the average spin orderings compensate along the y direction. Furthermore, projections of unequal magnitude (i.e., $M_z^{\alpha}+L_{3z}^{\alpha}$ and $M_z^{\alpha+}-2L_{1z}^{\alpha}-L_{3z}^{\alpha}$) are found along the z direction, as well as between the x, y, and z directions.

Such results contradict the three-sublattice arrangement proposed by von Wartburg from neutron diffraction data.[83] The magnetic structure suggested by this author consists of three antiferromagnetic orthorhombic sublattices: Only one, parallel to the y direction, is ferromagnetically ordered and responsible for the total magnetization, the two others being strictly antiferromagnetic and lying in the xy plane. An essential difference with our model is that, in Ref. 83, the same magnitude is assumed for all the spins which are distributed within an orthorhombic cell. A neutron diffraction experiment reinvestigating the low temperature phase of Ni-I boracite

would be suitable in order to verify the monoclinicity of the magnetic structure and the corresponding ordering which satisfies Eqs. (31).

B. One-dimensional weak ferromagnetism in trigonal boracites

The trigonal cell in Fe-X and Co-Cl boracites was reported to be equitranslational with the cubic phase.[9] It thus contains two formula units, i.e., six metal ions, the coordinates of which are given in Table X. As the magnetic transition occurs without a multiplication of the paramagnetic cell (see Sec. II), the magnetic structure will be determined by assigning the mean spins s_i $(i=1-6)$ of each of the six magnetic ions (e.g., Fe^{2+} or Co^{2+}). The location of the metallic ions, denoted 1 to 6, is shown on Fig. 10.

The transformation properties of the s_i under the effect of the paramagnetic group $R3c1'$ operations allow to introduce the vectors M and L_i $(i=1-3)$, defined by the equalities

$$\begin{aligned} L_1 &= -\tfrac{1}{2}(2s_1-s_2-s_3)+(\sqrt{3}/2)(2s_4-s_5-s_6)\ , \\ L_2 &= (\sqrt{3}/2)(2s_1-s_2-s_3)-\tfrac{1}{2}(2s_4-s_5-s_6)\ , \\ L_3 &= s_1+s_2+s_3-s_4-s_5-s_6\ , \\ M &= s_1+s_2+s_3+s_4+s_5+s_6\ , \end{aligned} \tag{32}$$

where M is the mean magnetic moment of the unit cell, and the L_i antiferromagnetic vectors. The components of these vectors span a reducible corepresentation of the $R3c1'$ group, which decomposes into the three IC's of the same group at the Brillouin-zone center $\Gamma(\mathbf{k}_7=\mathbf{0})$ (see Table II). The one-dimensional IC's, τ_1 and τ_2, transform according to the components L_{3z} and M_z, respectively, whereas the two-dimensional IC, labeled τ_3 in Table II, is spanned by L_{ix},L_{iy} $(i=1,2)$ as well as by $M_x,-M_y$. Thus, the order parameter (η_1,η_2) associated to the $R3c1'\rightarrow m$ transition identifies with the antiferromagnetic projections (L_{1x},L_{2y}). Let us write the corresponding Landau expansion as a function of M and L_{iu} $(u=x,y,z)$:

$$\begin{aligned} F=&\frac{a}{2}(L_1^2+L_2^2)+\frac{B}{4}(L_1^4+L_2^4)+\frac{C}{6}(L_1^6+L_2^6)+\frac{C}{2}M^2 \\ &+DM^2L^2+\left[\frac{\mu_1}{2}M_xM_y+\frac{\mu_2}{2}M_z^2\right](L_1^2+L_2^2) \\ &+\frac{\alpha}{2}L_{3z}^2+\frac{b}{2}M_z^2+\frac{\alpha}{2}(L_{1x}^2+L_{2y}^2)+\frac{\beta}{4}(L_{1x}^4+L_{2y}^4) \\ &+\frac{\gamma}{6}(L_{1x}^6+L_{2y}^6)+\delta(L_{1x}M_y-L_{2y}M_x)\ . \end{aligned} \tag{33}$$

In (33) we have written, in the following order, the terms representing exchange interactions, mixed exchange-relativistic terms (i.e., the μ_i invariants), and relativistic terms corresponding to the magnetic anisotropy of the crystal. As noted in Sec. IV, it is the presence of the δ coupling term of relativistic origin which determines the existence of the spontaneous magnetization below T_c, and thus the weak ferromagnetic character of the transition. On the other hand, it is the "twice relativistic" γ term[46] which is responsible for the symmetry breaking below T_c.

TABLE X. Coordinates of the metallic ions associated with the six average spins s_i $(i=1-6)$ in the trigonal $R3c$ phase of boracites. Hexagonal coordinates are used.

s_1:	x,y,z
s_2:	$\bar{y},x-y,z$
s_3:	$y-x,\bar{x},z$
s_4:	$\bar{y},\bar{x},\frac{1}{2}+z$
s_5:	$x,x-y,\frac{1}{2}+z$
s_6:	$y-x,y,\frac{1}{2}+z$

The equilibrium equations for the low-temperature phases are

$$L_{3z}=0,\quad M_z=0,\quad M_x=\frac{\delta}{C}L_{2y},\quad M_y=-\frac{\delta}{C}L_{1x}\ . \tag{34}$$

The monoclinic phase of symmetry Cc found in trigonal boracites corresponds to $L_{1x}\neq 0, L_{2y}=0$. Accordingly, the magnetization vector lies along the y axis, the proportionality coefficient δ/C being of the order of 10^{-2}–10^{-5}. In Table IX it can be seen that the experimental values found for the weak magnetization as percentages of the maximum magnetization, when all the magnetic moments are parallel in the compounds, extend from 3×10^{-2} for Fe-I boracite, to 8.7×10^{-2} for Co-Cl

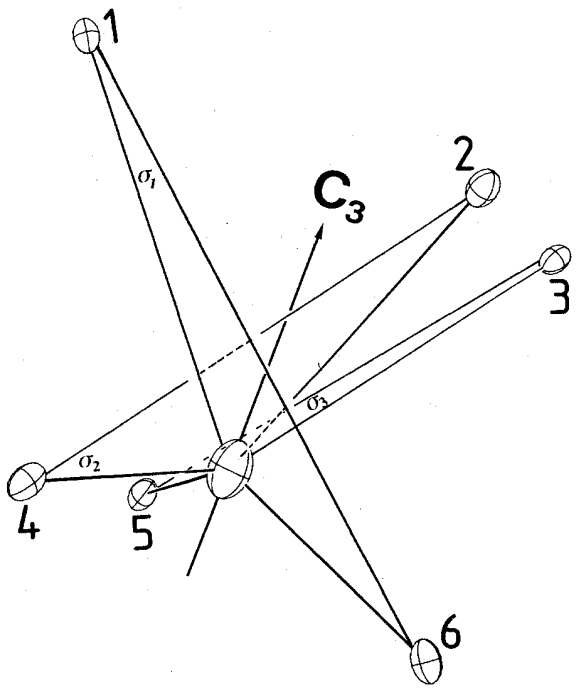

FIG. 10. Position in space for the six metallic ions in the trigonal boracite cell, with respect to the symmetry operations of the $R3c$ unit cell.

boracite. This order of magnitude is larger than the theoretical prediction,[46] and also than the values reported for standard weak ferromagnets, namely $\sim 10^{-3}$ for α-Fe_2O_3, $\sim 7\times 10^{-3}$ for $MnCO_3$, and $\sim 1\times 10^{-2}$ for C_2F_3.[102] The first-order character assumed for the transitions (see Sec. IV), as well as a possible influence of the coupling to the polarization may explain such large values found for the magnetization in the trigonal boracite series.

Introducing Eqs. (34) in (32) yields

$$\begin{aligned} &s_{1z}+s_{2z}+s_{3z}=s_{4z}+s_{5z}+s_{6z}=0\ , \\ &\sqrt{3}(2s_{1y}-s_{2y}-s_{3y})-(2s_{4y}-s_{5y}-s_{6y})=0\ , \\ &-(2s_{1x}-s_{2x}-s_{3x})+\sqrt{3}(2s_{4x}-s_{5x}-s_{6x})\neq 0\ . \end{aligned} \tag{35}$$

Equations (35) express that the mean spins s_i do not compensate in the x direction, but are turned with respect to each other by a small canting angle, of about 10^{-2}, giving rise to a weak ferromagnetic moment along the perpendicular direction y. As in Ref. 46, more detailed informations could be obtained from the model, by taking into account the influence of the higher degree invariants in (33). However, such predictions are of little interest in the absence of more detailed experimental data on the magnetic structure of the monoclinic phase.

C. One- or two-dimensional antiferromagnetism and weak ferromagnetism in orthorhombic boracites

In the orthorhombic $Pca2_1$ cell of boracites, the 12 metallic ions split into three independent sublattices.[7] In each sublattice the symmetry elements of the group transform the four atoms into each other (Fig. 11). Denoting s_1,s_2,s_3,s_4; $s_i'=s_{i+4}$; $s_i''=s_{i+8}$ $(i=1-4)$, the mean spins of the 12 ions (Table XI), one can define the four vectors

$$\begin{aligned} L_1&=(s_1+s_1'+s_1'')-(s_2+s_2'+s_2'')+(s_3+s_3'+s_3'')\\ &\quad-(s_4+s_4'+s_4'')\ , \\ L_2&=(s_1+s_1'+s_1'')+(s_2+s_2'+s_2'')-(s_3+s_3'+s_3'')\\ &\quad-(s_4+s_4'+s_4'')\ , \\ L_3&=(s_1+s_1'+s_1'')-(s_2+s_2'+s_2'')-(s_3+s_3'+s_3'')\\ &\quad+(s_4+s_4'+s_4'')\ , \\ M&=\sum_i (s_i+s_i'+s_i'')\ . \end{aligned} \tag{36}$$

TABLE XI. Coordinates of the metallic ions associated with the 12 average spins s_i,s_i',s_i'' $(i=1-4)$ in the orthorhombic $Pca2_1$ phase of boracites, with reference to the cubic axes.

s_1: $\frac{3}{4},\frac{1}{4},\frac{1}{2}$	s_1': $\frac{3}{4},\frac{1}{2},\frac{1}{4}$	s_1'': $0,\frac{1}{4},\frac{1}{4}$
s_2: $\frac{1}{4},\frac{1}{4},0$	s_2': $\frac{3}{4},\frac{1}{2},\frac{3}{4}$	s_2'': $0,\frac{1}{4},\frac{3}{4}$
s_3: $\frac{1}{4},\frac{1}{4},\frac{1}{2}$	s_3': $0,\frac{3}{4},\frac{1}{4}$	s_3'': $\frac{1}{4},\frac{1}{2},\frac{1}{4}$
s_4: $\frac{3}{4},\frac{1}{4},0$	s_4': $0,\frac{3}{4},\frac{3}{4}$	s_4'': $\frac{1}{4},\frac{1}{2},\frac{3}{4}$

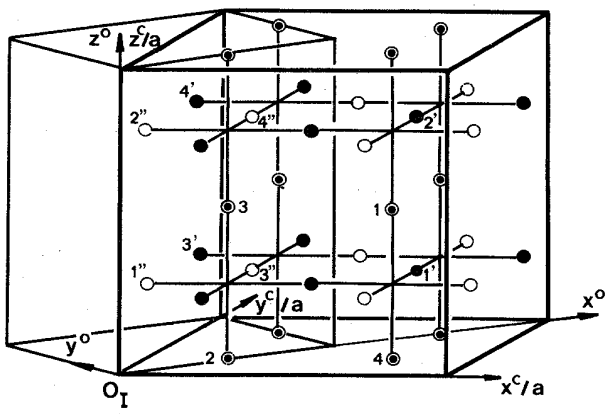

FIG. 11. Position of the 12 metallic ions in the orthorhombic $Pca2_1$ boracite cell. The orthorhombic (x^0,y^0,z^0) and cubic axes have the same origin (O_I) as in Ref. 5.

M, L_1, L_2, and L_3 form a basis of the four one-dimensional IC's, labeled τ_1 to τ_4 in Table II, of the $Pca2_11'$ group, at the center of the primitive orthorhombic Brillouin zone. From the transformation properties of the s_i,s_i',s_i'', one can find that the preceding IC's have the symmetry properties of the components (L_{1x},L_{2y},L_{3z}) for τ_1, (M_z,L_{1y},L_{2x}) for τ_2, (M_x,L_{2z},L_{3y}) for τ_3, and (M_y,L_{1z},L_{3x}) for τ_4. The Landau expansion associated with the four-dimensional reducible corepresentation $\tau_1+\tau_2+\tau_3+\tau_4$ can be written as a function of M,L_i,M_u,L_{iu} $(i=1-3,\ u=x,y,z)$:

$$\begin{aligned} F=&\sum_i(\tfrac{1}{2}a_iL_i^2+\tfrac{1}{4}B_iL_i^4)+\tfrac{1}{2}CM^2\\ &+\tfrac{1}{2}\sum_{i,u}\alpha_{iu}L_{iu}^2+\delta_1L_{1x}L_{2y}+\delta_2L_{1x}L_{3z}+\delta_3L_{2y}L_{3z}\\ &+\delta_4L_{1y}L_{2x}+\delta_5L_{2z}L_{3y}+\delta_6L_{1z}L_{3x}+\delta_1'M_xL_{2z}\\ &+\delta_2'M_xL_{3y}+\delta_3'M_yL_{1z}+\delta_4'M_yL_{3x}\\ &+\delta_5'M_zL_{1y}+\delta_6'M_zL_{2x}\ . \end{aligned} \tag{37}$$

For the sake of brevity, higher-degree relativistic terms, as well as mixed exchange-relativistic terms have been omitted from (37). The relativistic δ_i and δ_i' terms account for the coupling of the L_{iu} with the M_u and $L_{u'\neq u}$, respectively. In particular, it is the δ_i' coupling terms which lead to the appearance of the weak magnetization components of relativistic nature.

In the paramagnetic phase $Pca2_11'$, every a_i, $B>0$, and the minimum of F corresponds to the state in which all the L_i and M are equal to zero. A transition takes place when one of the a_i or B becomes zero. Minimization of F shows that a variety of antiferromagnetic, ferromagnetic, or weak ferromagnetic phases may occur depending on the values of the coefficients in (37). For example, let us assume that a_3 becomes zero at T_c with a_1, a_2, and $B>0$. Neglecting the relativistic terms in (37) yields

$$L_3 \neq 0, \quad L_1 = L_2 = M = 0 . \tag{38}$$

Introducing (38) into (36) yields

$$(s_1 + s_1' + s_1'') = (s_4 + s_4' + s_4'') = -(s_2 + s_2' + s_2'') = -(s_3 + s_3' + s_3'') . \tag{39}$$

Consequently, an antiferromagnetic spin distribution of purely exchange origin, described by the vector L_3, takes place below T_c. However, in reality one has to take into account the relativistic terms in (37). One finds then that depending on the respective magnitude of the coefficients α_{3x}, α_{3y}, and α_{3z}, the low-temperature phase will display the symmetries $Pca'2_1'$, $Pc'a2_1'$, or $Pca2_1$. The magnetic group $Pca'2_1'$ allows the existence of a weak magnetic moment $M_y = -(a_3/\delta_4')L_{3x}$, which results from a canting of the spins aligned along the x direction. A similar situation corresponds to the symmetry $Pc'a2_1'$, with a nonzero magnetic moment $M_x = -(a_3/\delta_2')L_{3y}$ due to a small angle between the spins pointing along the y direction. By contrast, the $Pca2_1$ group is associated with a strictly compensated antiferromagnetic structure.

Similarly, one can discuss the different situations arising when a_1, a_2, or B vanish first. In particular, in the case $B=0$, $a_i > 0$, one should observe normal exchange ferromagnetism. Below we shall restrict ourselves to enumerate briefly the situations of interest for the present study, i.e., which have been observed in orthorhombic boracites.

(i) The antiferromagnetic phase of symmetry $Pca2_1$ observed in Ni-Cl boracite may correspond *a priori* to one of the three possibilities: $L_i \neq 0$. However, the experimental data, which suggest an antiferromagnetic ordering along the z direction (see Sec. V), speak in favor of $L_3 \neq 0$, $L_1 = L_2 = 0$. Thus the spin distribution should verify Eqs. (39) with a strictly compensating exchange antiferromagnetism. L_3 reduces to its component $L_{3z} = 4(s_{1z} + s_{1z}' + s_{1z}'')$.

(ii) In the weak ferromagnetic phase of symmetry $Pc'a'2_1$ reported for Cu-Cl, the weak magnetization of relativistic origin is equal to $M_z = (a_1/\delta_5')L_{1y} - (a_2/\delta_6')L_{2x}$. Here one has $L_3 = 0$, $L_{1x} = L_{3x} = L_{2y} = L_{3y} = 0$. Thus, from (36) one obtains

$$(s_1 + s_1' + s_1'') = -(s_4 + s_4' + s_4'') ,$$
$$(s_2 + s_2' + s_2'') = -(s_3 + s_3' + s_3'') ,$$
$$L_{1y} = 2(s_{1y} + s_{1y}' + s_{1y}'') - 2(s_{2y} + s_{2y}' + s_{2y}'') ,$$
$$L_{2x} = 2(s_{1x} + s_{1x}' + s_{1x}'') - 2(s_{3x} + s_{3x}' + s_{3x}'') .$$

Accordingly, the noncompensation of the components L_{1y} and L_{2x} results from a canting angle with respect to the xy plane.

(iii) If one assumes M_y to be the weak magnetization component observed in Ni-Cl, Ni-Br, and Co-Br (the case where $M_x \neq 0$, $M_y = 0$ is treated equivalently), one finds the antiferromagnetic sublattices to lie in the xz plane. M_y is a linear combination of $(a_1/\delta_3')L_{1z}$ and $(a_3/\delta_4')L_{3x}$. Introducing in (36) the equalities $M=0$, $L_2=0$ yields

$$(s_1 + s_1' + s_1'') = -(s_2 + s_2' + s_2'') ,$$
$$(s_3 + s_3' + s_3'') = -(s_4 + s_4' + s_4'') ,$$
$$L_{1z} = 2(s_{3z} + s_{3z}' + s_{3z}'') - 2(s_{2z} + s_{2z}' + s_{2z}'') ,$$
$$L_{3x} = 2(s_{4x} + s_{4x}' + s_{4x}'') - 2(s_{2x} + s_{2x}' + s_{2x}'') .$$

The s_i are thus canted with respect to the xz plane.

Finally, let us note that the experimental values found for the weak magnetization in orthorhombic boracites extend from 0.08 G in Cu-Cl, to 482 G in Co-Br (Table IX). With the exception of Co-Br, it corresponds to a ratio of the magnetization to the nominal saturation moment, which is in the range of the numbers expected for weak ferromagnets: from 5×10^{-4} for Cu-Cl, to 2×10^{-2} for Co-I boracite. In Co-Br this ratio is 10^{-1}, i.e., the largest found in boracites. Actually a large canting angle appears from Table IX to be an intrinsic property of all cobalt boracites. The neutron-diffraction data available for Co-I boracite[84] do not give any information in this respect.

VII. CONCLUDING REMARKS

In this paper a phenomenological theory of the magnetic and magnetoelectric properties of boracites has been developed. An interpretation has been proposed for the main distinctive features characterizing the transitions in this family of compounds, namely the symmetry changes, the magnetic and magnetoelectric anomalies, the nature of the order parameter and its relationship with the relevant macroscopic components arising below T_c. Two situations, differing in an essential manner on a physical basis, have been distinguished. They occur respectively in Ni-I boracite, and in the other ten members of the boracite family considered in this study.

Ni-I boracite displays exceptional features which make it unique not only among boracities, but more generally among all known materials undergoing a magnetic *or* structural transition. It was already known to be the only system in which ferromagnetic, ferroelectric, and ferroelastic properties appear simultaneously and directly coupled. Our analysis has revealed that this material concretizes a number of special peculiarities which can be predicted on a theoretical basis. (i) The simultaneity of its magnetic and structural modifications is not accidental but can be foreseen from the symmetry of its order parameter. Thus, the onset of spontaneous components of the magnetization, polarization, and strain tensors originate in a nonlinear coupling to the order parameter, in such a way that the magnetic properties cannot establish if the structural modifications do not take place. (ii) The symmetry group of the low-temperature phase is a nonmaximal subgroup of the paramagnetic cubic group. Accordingly, Ni-I boracite is the first experimental example contradicting the maximal subgroup rule, usually admitted for phase transitions described by an order parameter. (iii) The weak magnetization component found in Ni-I boracite, results from a noncompensation of the antiferromagnetic ordering, identified as the primary transition

order parameter, through a mechanism involving exchange forces. The corresponding "latent" antiferromagnetic structure is formed by antiparallel average spins of different magnitude, associated with only one type of identical magnetic ions, which is found in equivalent crystallographic positions in the paramagnetic phase. Such a magnetic ordering has distinctive macroscopic features, namely a $M \sim (T_c - T)^{3/2}$ temperature variation for the magnetization in the vicinity of T_c, a weak value for M, and the existence of a simultaneous structural ordering.

An interesting theoretical property of Ni-I boracite could be added to the preceding enumeration. The Landau-Wilson Hamiltonian associated with its six-dimensional order-parameter expansion was shown, in another framework,[110,117,118] to have no stable fixed point of the renormalization group recursion relations. Several authors[108,119] have hypothesized that the lack of stable fixed points for a given system, was a sufficient condition for a transition taking place in this system to be first order. The discussion of the observed anomalies in Ni-I boracite have shown that most of the features in this compound suggest a *continuous* character for its 61.5-K transition. If this fact receives confirmation, Ni-I boracite would provide a counterexample to the above-mentioned conjecture.

The transitions in the other magnetic boracites have been treated as essentially magnetic modifications, their magnetoelectric and magnetoelastic properties being due to secondary couplings between the spontaneous magnetic quantities and the corresponding nonspontaneous polar tensors. A symmetry analysis of the phase sequences, has shown that two subclasses of compounds could be distinguished owing, respectively, to their trigonal or orthorhombic "parent" phase. The transitions in trigonal boracites appear to follow a single scheme with the same two-component order-parameter symmetry. By contrast, the variety of phases evidenced in orthorhombic boracites, can be related to four different one component order parameters. In the two groups of compounds, it is a bilinear coupling between the order parameter and the magnetization which gives rise to a weak ferromagnetic component of relativistic origin.

The present theory of magnetic boracites has allowed to illustrate the link existing between two, formally different, Landau-type approaches of phase transitions. On one hand, the phenomenological description of the symmetry changes and transition anomalies, usually performed for structural transitions,[36,38,39] and based on the concepts of improper or pseudoproper transitions, and on the other hand, the semimicroscopic approach, introduced by Dzialoshinskii[46,47,105] for magnetic systems, which allows to deduce the fundamental forces responsible for a magnetic ordering.

In the Introduction, the variety of situations found in the magnetic properties of boracites was stressed. Although a number of questions remain to be settled experimentally as well as theoretically, our analysis has brought some coherency to the observed behaviors. It has also illustrated the capability of the Landau method, to clarify the macroscopic behavior of systems possessing strong anisotropies and a large number of degrees of freedom.

ACKNOWLEDGMENTS

We are grateful to Professor P. Fischer, Professor K. Kohn, and Professor M. Haida for allowing us to quote from their unpublished results. This work has benefited from very helpful discussions with L. N. Baturov, I. E. Dzialoshinskii, A. P. Levanyuk, Yu. M. Gufan, O. V. Kovalev, D. G. Sannikov, G. Berset, W. Depmeier, and M. E. Mendoza-Alvarez. Dr. J. C. Tolédano has clarified for us a number of group-theoretical aspects of the Dzialoshinskii approach. It is a pleasure to thank Dr. A. F. Williams for a careful reading of the manuscript. The work was supported by the Swiss National Science Foundation (Contract Nos. 2.833-0.83 and 2.231-0.84), and by the Troisième cycle de l'Enseignement de la Chimie en Suisse Romande.

APPENDIX A

In the Landau theory of magnetic transitions, the symmetry change which takes place at a continuous transition, is determined by the symmetry properties of the transition order parameter, whose n components span an n-dimensional irreducible corepresentation of the high-symmetry group G_0. More precisely, the space group G of the low-symmetry phase coincides with the complete set of symmetry operations belonging to G_0 and leaving invariant the vector

$$\delta\rho = \sum_{i=1}^{n} \eta_i^0 \psi_i \ ,$$

where the ψ_i constitute a basis of the abstract vector space ϵ of the corepresentation. The η_i^0 coefficients are particular values of the order-parameter components η_i corresponding to the absolute minimum of the order-parameter expansion $F_1(\eta_i, \alpha, \beta_k)$ where $\alpha \sim (T - T_c)$ is the coefficient of the quadratic term, and the β_k are the coefficients of the independent homogeneous polynomials of higher degrees. For $n > 2$ depending on the relative algebraic values of the β_k the absolute minimum of F, below the transition can correspond to various vector directions $\delta\rho_i \in \epsilon$, generally associated with distinct low-symmetry groups G_i. To enumerate the set of possible G_i groups compatible with the considered order parameter, one has therefore to locate, for the whole range of the β_k values all the directions $\delta\rho_i$ making F_1 to be an absolute minimum, and for each such direction to identify its invariance group G_i, subgroup of G_0. The possible low-symmetry groups are therefore the entire set $\{G_i\}$ of invariance groups of all the directions $\delta\rho_i \in \epsilon$. Several authors[72,74] have attempted to avoid the minimization of F, and have conjectured that the preceding $\delta\rho_i$ directions could be selected on the basis of symmetry considerations. Thus, it was stated by Ascher[72] that the directions $\delta\rho_i \in \epsilon$ corresponding to the absolute minimum of F were the ones having an invariance group G_i^m constituting a *maximal* subgroup of G_0. If we consider the set $\{G_i\}$ specified above, the maximal subgroups are defined by the following conditions:

$$G_i^m \subset \{G_i\} \quad \text{and} \quad G_i^m \not\subset G_j \in \{G_i\} \ .$$

In other terms, if G_1 and G_2 are, respectively, the invariance groups of $\delta\rho_1$ and $\delta\rho_2 \in \epsilon$, with $G_2 \subset G_1 \subset G_0$, then the direction $\delta\rho_2$ cannot correspond to the absolute minimum of F, for any set of values of the β_k coefficients.

The Landau expansion $d(\rho_i,\psi_i,\beta_k)$ associated with the six-dimensional IC $\tau_1(X)$ of the $F\bar{4}3c\,1'$, possesses *eight absolute minima* for $\alpha<0$. For each of the corresponding stable phases, the equilibrium values for the ρ_i, ψ_i, and range of values for the β_k, are given in Table III. The invariance groups G_i associated with the directions $\delta\rho_i$ labeled I to VI are *maximal subgroups* of $F43c\,1'$. Thus, one can verify: (i) that each G_i corresponds to the maximal number of matrices of τ_1 leaving invariant the direction $\delta\rho_i$; (ii) that the $G_i=\{P_1c2_1a(2v),C_A222_1(2V),P\bar{4}2_1c(4V),P2_13(4V),R3c(4V),R3c'(4V)\}$ are not related to one another by any group subgroup relationship.

By contrast, the G_i corresponding to the direction denoted VII and VIII in Table III are nonmaximal subgroups of $F43c\,1'$. This can easily be foreseen as $Cc'(4V)\subset R3c'(4V)$ (direction VII) and $Cc(4V)\subset R3c(4V)$ (direction VIII). It can be noted that the range of values for the β_k coefficients for the VII and VIII directions are *included* in the ranges of values of the β_k corresponding, respectively, to the directions VI ($R3c'$) and V ($R3c$). In these restricted intervals the monoclinic phases are *more stable* than the corresponding rhombohedral phases (i.e., they are associated with an *absolute* minimum of the free energy F).

APPENDIX B

In this appendix, we give for each of the IC's which have been shown (Sec. II) to be connected with the magnetic transitions in boracites: (a) the coordinates of the **k** vectors belonging to the relevant star $\mathbf{k}^*$; (b) the corresponding group of the **k** vector; (c) the generative matrices of the IC. The notation of the Kovalev tables[109] is used.

(1) For $F\bar{4}3c\,1'$, τ_1 ($X\equiv\mathbf{k}_{10}$):

(a) $\mathbf{k}_1=(0,0,\pi/a)$, $\mathbf{k}_2=(0,\pi/a,0)$, $\mathbf{k}_3=(\pi/a,0,0)$;

(b) $G_{k_1}=I\bar{4}c\,21'$;

(c)

$(U_z\,|\,000)$

$$\begin{bmatrix} -1 & 0 & & & \\ 0 & -1 & & \underline{0} & \\ & & 0 & -1 & \\ & \underline{0} & -1 & 0 & \\ & & & & 0\ 1 \\ & \underline{0} & & \underline{0} & 1\ 0 \end{bmatrix}$$

$(U_y\,|\,000)$

$$\begin{bmatrix} 0 & -1 & & & \\ -1 & 0 & & \underline{0} & \\ & & 0 & 1 & \\ & \underline{0} & 1 & 0 & \\ & & & & -1\ 0 \\ & \underline{0} & & \underline{0} & 0\ -1 \end{bmatrix}$$

$(S_4^z\,|\,00\,\frac{1}{2}a)$

$$\begin{bmatrix} 0 & -1 & & & \\ 1 & 0 & & \underline{0} & \\ & & 1 & 0 & \\ & \underline{0} & 0 & -1 & \\ & & & & 0\ 1 \\ & \underline{0} & & \underline{0} & -1\ 0 \end{bmatrix}$$

$(C_3^{xyz}\,|\,000)$

$$\begin{bmatrix} & & 1 & 0 & \\ & \underline{0} & 0 & 1 & \underline{0} \\ & & & & 1\ 0 \\ & \underline{0} & & \underline{0} & 0\ 1 \\ 1 & 0 & & & \\ 0 & 1 & \underline{0} & & \underline{0} \end{bmatrix}$$

t_2

$$\begin{bmatrix} -1 & 0 & & & \\ 0 & -1 & & \underline{0} & \\ & & 1 & 0 & \\ & \underline{0} & 0 & 1 & \underline{0} \\ & & & & -1\ 0 \\ & \underline{0} & & \underline{0} & 0\ -1 \end{bmatrix}$$

t_3

$$\begin{bmatrix} 1 & 0 & & & \\ 0 & 1 & & \underline{0} & \\ & & -1 & 0 & \\ & \underline{0} & 0 & -1 & \underline{0} \\ & & & & -1\ 0 \\ & \underline{0} & & \underline{0} & 0\ -1 \end{bmatrix}$$

RE

$$\begin{bmatrix} -1 & 0 & & & \\ 0 & -1 & & \underline{0} & \\ & & -1 & 0 & \\ & \underline{0} & 0 & -1 & \underline{0} \\ & & & & -1\ 0 \\ & \underline{0} & & \underline{0} & 0\ -1 \end{bmatrix}$$

t_1

$$\begin{bmatrix} -1 & 0 & & & \\ 0 & -1 & & \underline{0} & \\ & & -1 & 0 & \\ & \underline{0} & 0 & -1 & \underline{0} \\ & & & & 1\ 0 \\ & \underline{0} & & \underline{0} & 0\ 1 \end{bmatrix}$$

(2) For $R3c\,1'$, τ_3 ($\Gamma\equiv\mathbf{k}_7$):

(a) $\mathbf{k}=(0,0,0)$;

(b) $G_k=R3c\,1'$;

(c)	$(C_3 \mid 000)$	$(\sigma_{\bar{x}y} \mid 00\frac{3}{2}c)$	RE	t_1,t_2,t_3
τ_1	1	-1	-1	1
τ_2	1	-1	-1	1
τ_3	$\begin{bmatrix} -1/2 & -\sqrt{3}/2 \\ \sqrt{3}/2 & -1/2 \end{bmatrix}$	$\begin{bmatrix} 0 & 1 \\ 1 & 0 \end{bmatrix}$	$\begin{bmatrix} -1 & 0 \\ 0 & -1 \end{bmatrix}$	$\begin{bmatrix} 1 & 0 \\ 0 & 1 \end{bmatrix}$

(3) For $Pca2_11'$, $\tau_1 \rightarrow \tau_4$ ($\Gamma \equiv \mathbf{k}_{19}$):

(a) $\mathbf{k}=(0,0,0)$;

(b) $G_k = Pca2_11'$;

(c)	$(E \mid 000)$	$(U_z \mid 00\frac{1}{2}c)$	$(\sigma_x \mid \frac{1}{2}a\,0\,\frac{1}{2}c)$	$(\sigma_y \mid \frac{1}{2}a\,00)$	RE	t_1,t_2,t_3
τ_1	1	1	1	1	-1	1
τ_2	1	1	-1	-1	-1	1
τ_3	1	-1	1	-1	-1	1
τ_4	1	-1	-1	1	-1	1

*On leave from the University of Picardie 33 rue St. Leu, 80.000 Amiens, France.

[1]H. Schmid, J. Phys. Chem. Solids **26**, 973 (1965).
[2]E. Ascher, H. Schmid, and D. Tar, Solid State Commun. **2**, 45 (1964).
[3]H. Schmid, H. Rieder, and E. Ascher, Solid State Commun. **3**, 325 (1965).
[4]E. Ascher, H. Rieder, H. Schmid, and H. Stössel, J. Appl. Phys. **37**, 1404 (1966).
[5]T. Ito, N. Morimoto, and R. Sadanaga, Acta Crystallogr. **4**, 310 (1951).
[6]H. Schmid, Rost Krist. **7**, 32 (1969) [Growth Cryst. (USSR) **7**, 25 (1969)].
[7]E. Dowty and J. R. Clark, Z. Kristallogr. **138**, 64 (1973).
[8]G. Quézel and H. Schmid, Solid State Commun. **6**, 447 (1968).
[9]H. Schmid, Phys. Status Solidi **37**, 209 (1970).
[10]J. Kobayashi, I. Sato, and H. Schmid, Phys. Status Solidi A **10**, 259 (1972).
[11]J. P. Rivera, Ferroelectrics **21**, 455 (1978).
[12]M. E. Mendoza-Alvarez, J. P. Rivera, H. Schmid, and G. Wildermuth, Ferroelectrics **55**, 213 (1984).
[13]L. N. Baturov and B. I. Al'shin, Fiz. Tverd. Tela (Leningrad) **21**, 3 (1979) [Sov. Phys.—Solid State **21**, 1 (1979)].
[14]J. P. Rivera and H. Schmid, Ferroelectrics **36**, 447 (1981).
[15]W. A. Smith, M. E. Rosar, and A. Shaulov, Ferroelectrics **36**, 467 (1981).
[16]A. Shaulov, W. A. Smith, and H. Schmid, Ferroelectrics **34**, 219 (1981).
[17]S. N. Drozhdin, B. G. Bochkov, N. D. Gavrilova, T. V. Popova, V. A. Koptsik, and V. K. Novik, Kristallografiya **20**, 854 (1975) [Sov. Phys.—Crystallogr. **20**, 526 (1976)].
[18]Y. Le Corre, J. Phys. Radium **18**, 629 (1957).
[19]F. Smutny and J. Fousek, Phys. Status Solidi **40**, K13 (1970).
[20]J. P. Rivera and H. Schmid, Ferroelectrics **55**, 295 (1984).
[21]L. P. Torre, S. C. Abrahams, and R. L. Barns, Ferroelectrics **4**, 291 (1972).
[22]F. Smutny and C. Konak', Phys. Status Solidi **31**, 151 (1975).
[23]R. W. Whatmore, C. J. Brierley, and F. W. Ainger, Ferroelectrics **27**, 67 (1980).
[24]H. Schmid, P. Chan, L. A. Peterman, F. Teufel, and M. Mandly, Ferroelectrics **13**, 351 (1976).
[25]M. Delfino, G. M. Loiacono, W. A. Smith, and P. S. Gentile, J. Solid State Chem. **33**, 107 (1980).
[26]A. G. Castellanos-Guzman, J. C. Burfoot, H. Schmid, and P. Tissot, Ferroelectrics **36**, 411 (1981).
[27]P. Felix, M. Lambert, R. Comes, and H. Schmid, Ferroelectrics **7**, 131 (1974).
[28]P. Genequand, H. Schmid, G. Pouilly, and H. Tippman, J. Phys. (Paris) **39**, 287 (1978).
[29]M. E. Mendoza-Alvarez, H. Schmid, and J. P. Rivera, Ferroelectrics **55**, 227 (1984).
[30]I. H. Brunskill and H. Schmid, Ferroelectrics **36**, 395 (1981).
[31]L. N. Baturov, B. I. Al'shin, and D. N. Astrov, Fiz. Tverd. Tela (Leningrad) **19**, 916 (1977) [Sov. Phys.—Solid State **19**, 534 (1977)].
[32]J. P. Rivera, H. Schmid, J. P. Moret, and H. Bill, Int. J. Magn. **6**, 211 (1974).
[33]L. N. Baturov, R. V. Zorin, B. I. Al'shin, and V. I. Bugakov, Fiz. Tverd. Tela (Leningrad) **23**, 908 (1981) [Sov. Phys.—Solid State **23**, 525 (1981)].
[34]L. N. Baturov, R. V. Zorin, B. I. Al'shin, and Yu. N. Yarmukhamedov, Fiz. Tverd. Tela (Leningrad) **22**, 279 (1980) [Sov. Phys.—Solid State **22**, 166 (1980)].
[35]M. Haida, K. Kohn, and J. Kobayashi, J. Phys. Soc. Jpn. **39**, 1625 (1975).
[36]V. Dvorak and J. Petzelt, Czech. J. Phys. B **21**, 1141 (1971); V. Dvorak, *ibid.* B **21**, 1250 (1971).
[37]J. Kobayashi, Y. Enomoto, and Y. Sato, Phys. Status Solidi B **50**, 335 (1972).
[38]Yu. M. Gufan and V. P. Sakhnenko, Fiz. Tverd. Tela (Len-

ingrad) **14**, 1915 (1972) [Sov. Phys.—Solid State **14**, 1660 (1973)].
[39]A. P. Levanyuk and D. G. Sannikov, Fiz. Tverd. Tela (Leningrad) **17**, 526 (1975) [Sov. Phys.—Solid State **17**, 327 (1975)].
[40]Yu. M. Gufan, Zh. Eksp. Teor. Fiz. Pis'ma Red. **8**, 271 (1968) [JETP Lett. **8**, 167 (1968)].
[41]B. I. Al'shin, D. N. Astrov, and Yu. M. Gufan, Fiz. Tverd. Tela (Leningrad) **12**, 2666 (1970) [Sov. Phys.—Solid State **12**, 214 (1971)].
[42]O. V. Kovalev, Fiz. Tverd. Tela (Leningrad) **14**, 307 (1972) [Sov. Phys.—Solid State **14**, 258 (1972)].
[43]L. N. Baturov and B. I. Al'shin, Kristallografiya **25**, 781 (1980) [Sov. Phys.—Crystallogr. **25**, 448 (1981)].
[44]L. N. Baturov, N. A. Sokolov, and B. I. Al'shin, Fiz. Tverd. Tela (Leningrad) **25**, 1994 (1983) [Sov. Phys.—Solid State **25**, 1150 (1984)].
[45]M. Clin, M. Hédoux, and P. Toledano, Ferroelectrics **54**, 265 (1984).
[46]I. E. Dzialoshinskii, J. Exptl. Theoret. Phys. (U.S.S.R.) **32**, 1547 (1957) [Sov. Phys.—JETP **5**, 1259 (1957)].
[47]I. E. Dzialoshinskii and V. I. Man'ko, J. Exptl. Theoret. Phys. (U.S.S.R.) **46**, 1352 (1964) [Sov. Phys.—JETP **19**, 915 (1964)].
[48]J. P. Rivera and H. Schmid, Ferroelectrics **54**, 103 (1984).
[49]G. Will and H. Morche, J. Phys. C **10**, 1389 (1977).
[50]A. F. Murray and D. J. Lockwood, J. Phys. C **11**, 2349 (1978).
[51]W. Rehwald, J. Phys. C **11**, L157 (1978).
[52]A. F. Murray and D. J. Lockwood, J. Phys. C **11**, 4651 (1978).
[53]A. F. Kovalev and G. T. Andreeva, Fiz. Tverd. Tela (Leningrad) **21**, 1744 (1979) [Sov. Phys.—Solid State **21**, 999 (1979)].
[54]J. P. Rivera and H. Schmid, Ferroelectrics **42**, 35 (1982).
[55]J. Holakovsky and F. Smutny, J. Phys. C **11**, L611 (1978).
[56]H. Schmid, Int. J. Magn. **4**, 337 (1973).
[57]M. Haida, K. Kohn, and H. Schmid, J. Phys. Soc. Jpn. **37**, 1463 (1974).
[58]K. Kohn and M. Haida (unpublished); J. P. Rivera and H. Schmid (unpublished).
[59]M. E. Mendoza-Alvarez and H. Schmid (unpublished).
[60]In this paper, a fundamental distinction is made between (i) magnetostructural transitions, (ii) structural modifications induced by purely magnetic transitions. In the first case, *spontaneous* polar tensors (e.g., polarization, strain) arise simultaneously with the spontaneous magnetization. Both quantities transform as the same Brillouin-zone boundary irreducible representation, and the breaking of symmetry is both structural and magnetic. In case (ii), there is no spontaneous polar tensor arising at the magnetic transition, although the nonspontaneous polar tensors already existing in the high-temperature phase, may be affected by the magnetic transition. In this latter case the structural tensors transform as the identity irreducible representation, and thus are not symmetry breaking quantities.
[61]N. V. Belov, N. N. Neronova, and T. S. Smirnova, Kristallografiya **2**, 315 (1957) [Sov. Phys.—Crystallogr. **2**, 311 (1957)].
[62]E. P. Wigner, *Group Theory* (Academic, New York, 1959).
[63]C. J. Bradley and A. P. Cracknell, *The Mathematical Theory of Symmetry in Solids* (Clarendon, Oxford, 1972).
[64]O. V. Kovalev, Fiz. Tverd. Tela (Leningrad) **5**, 3156 (1963) [Sov. Phys.—Solid State **5**, 2309 (1964)].
[65]J. Sólyom, J. Phys. (Paris) Colloq. **32**, C1-471 (1971).
[66]A. P. Cracknell, J. Lorenc, and J. Przystava, J. Phys. C **9**, 1731 (1976).
[67]P. Tolédano, M. Clin, and M. Hédoux, Ferroelectrics **35**, 239 (1981).
[68]M. Clin, thèse de 3e cycle, Université de Paris VII, 1983) (unpublished); M. Clin and P. Tolédano (unpublished).
[69]G. Ya. Lyubarskii, *The Application of Group Theory in Physics* (Pergamon, New York, 1960).
[70]L. D. Landau and E. M. Lifshitz, *Statistical Physics* (Pergamon, Oxford, 1958).
[71]*International Tables for Crystallography,* edited by Theo. Hahn and D. Reidel (Reidel, Boston, 1983), Vol. A.
[72]E. Ascher, J. Phys. C **10**, 1365 (1977).
[73]J. C. Toledano and P. Tolédano, J. Phys. (Paris) **41**, 189 (1980).
[74]L. Michel and J. Mozrzymas, *Proceedings of the VI International Colloquium on Group Theoretical Methods in Physics, Tübingen (1977)* (Academic, New York, 1978).
[75]I. E. Chupis, Fiz. Nizk. Temp. **9**, 56 (1983) [Sov. J. Low Temp. Phys. **9**, 28 (1983)].
[76]P. Tolédano and G. Pascoli, Ferroelectrics **25**, 427 (1980).
[77]V. Janovec, V. Dvorak, and J. Petzelt, Czech. J. Phys. B **25**, 1362 (1975).
[78]V. Dvorak, Ferroelectrics **7**, 1 (1974).
[79]A. P. Levanyuk and D. G. Sannikov, Usp. Fiz. Nauk **112**, 561 (1974) [Sov. Phys.—Usp. **17**, 199 (1974)].
[80]I. E. Dzialoshinskii, J. Exptl. Theoret. Phys. (U.S.S.R.) **33**, 1454 (1957) [Sov. Phys.—JETP **6**, 1120 (1957)].
[81]S. A. Nikitin, Vestn. Mosk. Univ. Fiz., Asronomiya **6**, 664 (1970).
[82]W. Schäefer and G. Will, Phys. Status Solidi A **28**, 211 (1975).
[83]W. Von Wartburg, Phys. Status Solidi A **21**, 557 (1974).
[84]V. P. Plakhtii, A. V. Kovalev, M. N. Bedrizova, I. V. Golosovskii, and G. T. Andreeva, Fiz. Tverd. Tela (Leningrad) **18**, 2030 [Sov. Phys.—Solid State **18**, 1181 (1976)].
[85]G. A. Smolenskii and I. E. Chupis, Usp. Fiz. Nauk **137**, 415 (1982) [Sov. Phys.—Usp. **25**, 475 (1982)].
[86]R. E. Newnham, J. J. Kramer, W. A. Schulze, and L. E. Cross, J. Appl. Phys. **49**, 6088 (1978).
[87]If one assumes the spontaneous polarization P to be the primary order parameter, the spontaneous magnetization M arises as a secondary order parameter; the two quantities would be necessarily connected by a coupling term of the form $\delta P^n M$ with $n \geq 1$. Such a coupling is forbidden by the time-reversal operation belonging to the paramagnetic phase.
[88]K. Aizu, J. Phys. Soc. Jpn. **33**, 629 (1972).
[89]P. Fischer (unpublished).
[90]H. Schmid (unpublished).
[91]I. S. Zheludev, T. M. Perekalina, E. M. Smirnovskaya, S. S. Fonton, and Yu. N. Yarmukhamedov, Zh. Eksp. Teor. Fiz. Pis'ma Red. **20**, 289 (1974) [JETP Lett. **20**, 129 (1974)].
[92]T. Miyashita and T. Murakami, J. Phys. Soc. Jpn. **29**, 1092 (1970).
[93]L. E. Cross, A. Fouskova, and S. E. Cummins, Phys. Rev. Lett. **21**, 812 (1968).
[94]H. Schmid (unpublished).
[95]A. N. Holden, W. J. Merz, J. P. Remeika, and B. T. Mathias, Phys. Rev. **101**, 962 (1956).
[96]J. C. Toledano, Ann. Telecommun. **29**, 249 (1974).
[97]The assumed order of the path difference may have been erroneous due to the high absorption of the crystal.
[98]L. N. Baturov, B. I. Al'shin, and Yu. N. Yarmukhamedov, Fiz. Tverd. Tela (Leningrad) **20**, 2254 (1978) [Sov. Phys.—Solid State **20**, 1300 (1978)].
[99]J. P. Rivera and H. Schmid (unpublished).
[100]H. Schmid and L. A. Peterman, Phys. Status Solidi A **41**, K147 (1977).

[101]A. P. Cracknell, *Magnetism in Crystalline Materials* (Pergamon, Oxford, 1975).
[102]E. A. Turov, *Physical Properties of Magnetically Ordered Crystals* (Academic, New York, 1965).
[103]J. C. Toledano, Ann. Telecommun. **39**, 277 (1984).
[104]C. Kittel, *Introduction to Solid State Physics* (Wiley, New York, 1956).
[105]I. E. Dzialoshinskii, J. Exptl. Theoret. Phys. (U.S.S.R.) **46**, 1420 (1964) [Sov. Phys.—JETP **19**, 960 (1964)].
[106]O. V. Kovalev, Fiz. Tverd. Tela (Leningrad) **5**, 3164 (1963)] [Sov. Phys.—Solid State **5**, 2315 (1964)].
[107]A. Herpin, *Theorie du Magnétisme* (Presses Universitaires de France, Paris, 1968).
[108]S. A. Brazovskii, I. E. Dzialoshinskii, and B. G. Kukharenko, Zh. Eksp. Teor. Fiz. **70**, 2256 (1976) [Sov. Phys.—JETP **43**, 1178 (1976)].
[109]O. V. Kovalev, *Irreducible Representations of the Space Groups* (Gordon and Breach, New York, 1965).
[110]L. D. Landau and E. M. Lifshitz, *Electrodynamics of Continuous Media* (Addison-Wesley, Reading, 1960).
[111]L. D. Landau and E. M. Lifshitz, *Quantum Mechanics* (Pergamon, New York, 1965).
[112]T. O. Dell, H. Schmid, S. Shtrikman, and I. Yaeger (unpublished).
[113]E. W. Gorter, Philips Res. Rep. **9**, 403 (1954).
[114]E. F. Bertaut, F. Forret, A. Herpin, and P. Meriel, Rep. CEA **1**, 597 (1956).
[115]I. E. Dzialoshinskii and B. G. Kukharenko, Zh. Eksp. Teor. Fiz. **75**, 2190 (1978) [Sov. Phys.—JETP **48**, 1155 (1979)].
[116]I. E. Dzialoshinskii, Commun. Phys. **2**, 69 (1977).
[117]V. A. Alessandrini, A. P. Cracknell, and J. A. Przystawa, Commun. Phys. **1**, 51 (1976).
[118]D. Mukamel and S. Krinsky, Phys. Rev. B **13**, 5078 (1976).
[119]P. Bak, S. Krinsky, and D. Mukamel, Phys. Rev. Lett. **36**, 52 (1976).
[120]J. Zak, A. Cacher, M. Glück, and Y. Gür, *The Irreducible Representations of Space Groups* (Benjamin, New York, 1969).
[121]J. C. Tolédano and P. Tolédano, Phys. Rev. B **21**, 1139 (1980).